ENTATION PAGE

Form Approved
OMB No. 0704-0188

(2)

1. AGENCY USE ONLY (Leave blank)	2. REPORT DATE	3. REPORT TYPE AND DATES COVERED
	January 1993	Final Report 12/1/90-11/30/92

4. TITLE AND SUBTITLE
Mechanics of Elevated Temperature Fatigue Damage in Fiber-Reinforced Ceramics

5. FUNDING NUMBERS
61102F 2306/BS

6. AUTHOR(S)
John W. Holmes

7. PERFORMING ORGANIZATION NAME(S) AND ADDRESS(ES)
University of Michigan
475 East Jefferson Street
Ann Arbor, MI 48109-1248

8. PERFORMING ORGANIZATION REPORT NUMBER
2

9. SPONSORING/MONITORING AGENCY NAME(S) AND ADDRESS(ES)
AFOSR/NE
Building 410, Bolling AFB DC
20332-6448

10. SPONSORING/MONITORING AGENCY REPORT NUMBER
AFOSR-91-0106

11. SUPPLEMENTARY NOTES

12a. DISTRIBUTION/AVAILABILITY STATEMENT
APPROVED FOR PUBLIC RELEASE; DISTRIBUTION IS UNLIMITED.

12b. DISTRIBUTION CODE

13. ABSTRACT (Maximum 200 words)

The focus of the research conducted under Grant No. 91-0106 (a two year effort) was to identifying the fundamental mechanisms of fatigue damage that occur in fiber-reinforced ceramics. Several new findings were made during the research effort: (1) the fatigue life of fiber-reinforced ceramics decreased markedly during high frequency fatigue loading, (2) fiber-reinforced ceramics undergo significant internal heating during cyclic loading, (3) because of frictional wear along the fiber-matrix interface, the frictional shear stress in fiber-reinforced ceramics decreases sharply under cyclic loading. Based upon insight gained from the analytical and experimental parts of the investigation, we developed a novel approach to estimate the level of frictional shear stress that exists along the fiber-matrix interface during fatigue. Since this technique allows confirmation of other techniques for estimating frictional shear stress (e.g., fiber pushout technique developed by Marshall at Rockwell Science Center). Moreover, it is the only approach that allows determination of the in-situ change in frictional shear stress during cyclic loading (note that the level of frictional shear stress controls many mechanical properties such as strength, toughness and mechanical damping as well as thermophysical properties such as thermal diffusivity). The analysis that was developed to estimate frictional shear stress can also be used to understand the relationship between composite microstructure and cyclic energy dissipation in fiber-reinforced ceramics.

14. SUBJECT TERMS	15. NUMBER OF PAGES
93 062	72
	16. PRICE CODE

17. SECURITY CLASSIFICATION OF REPORT	18. SECURITY CLASSIFICATION OF THIS PAGE	19. SECURITY CLASSIFICATION OF ABSTRACT	20. LIMITATION OF ABSTRACT
UNCLASSIFIED	UNCLASSIFIED	UNCLASSIFIED	

MECHANICS OF ELEVATED TEMPERATURE FATIGUE DAMAGE IN FIBER-REINFORCED CERAMICS

AFOSR Grant No. 91-0106
Report for the funding period Dec. 90 to Dec. 92
Principal Investigator: John W. Holmes

The University of Michigan
Ceramics Composites Research Laboratory
Department of Mechanical Engineering
2250 G.G. Brown
Ann Arbor, MI 48109-2125

Table of Contents

I. Overview of Research Results

The focus of the research conducted under Grant No. 91-0106 (a two year effort) was to identifying the fundamental mechanisms of fatigue damage that occur in fiber-reinforced ceramics. Several new findings were made during the research effort: (1) the fatigue life of fiber-reinforced ceramics decreases markedly during high frequency fatigue loading, (2) fiber-reinforced ceramics undergo significant internal heating during cyclic loading, (3) because of frictional wear along the fiber-matrix interface, the frictional shear stress in fiber-reinforced ceramics decreases sharply under cyclic loading. Based upon insight gained from the analytical and experimental parts of the investigation, we developed a novel approach to estimate the level of frictional shear stress that exists along the fiber-matrix interface during fatigue. Since this technique allows confirmation of other techniques for estimating frictional shear stress (e.g., fiber pushout technique developed by Marshall at Rockwell Science Center). Moreover, it is the only approach that allows determination of the in-situ change in frictional shear stress during cyclic loading (note that the level of frictional shear stress controls many mechanical properties such as strength, toughness and mechanical damping as well as thermophysical properties such as thermal diffusivity). The analysis that was developed to estimate frictional shear stress can also be used to understand the relationship between composite microstructure and cyclic energy dissipation in fiber-reinforced ceramics.

For convenience, this report is divided into three sections that provide a detailed account of the research results. The first section discusses the influence of loading frequency on the room temperature fatigue life of Nicalon/CAS composites; these results were obtained after the 1991 progress report. The second and third sections discuss experimental results that show the magnitude and mechanisms of frictional heating in fiber-reinforced ceramics, and the approach that was developed to estimate the frictional shear stress that exists during fatigue loading of composites.

II. Dissemination of Research Results

A list of the publications, conference presentations and invited talks that were the direct result of this AFOSR project are listed below.

Journal Publications

1. C. Cho, J. W. Holmes and J. R. Barber, "Estimation of Interfacial Shear in Ceramic Composites from Frictional Heating Measurements," *J. Am. Ceram. Soc.*, **74** [11] 2802-2808 (1991).

2. J. W. Holmes and C. Cho, "Frictional Heating in a Unidirectional Fiber-Reinforced Ceramic Composite," *J. Mat. Sci. Lett.*, **11** (1992) 41-44.

3. C. Cho, J. W. Holmes, and J. R. Barber, "Distribution of Matrix Cracks in a Uniaxial Composite," *J. Am. Ceram. Soc.*, **75** [2] 316-24 (1992).

4. J. W. Holmes and C. Cho, "Experimental Observations of Frictional Heating in a Fiber Reinforced Ceramic," *J. Am. Ceram. Soc.*, **75** [4] 929-38 (1992).

5. L. Butkus*, J. W. Holmes and T. Nicholas, "Thermomechanical Fatigue of a SiC-Fiber Calcium Aluminosilicate Matrix Composite," *J. Am. Ceram. Soc.*, in press.

6. S. F. Shuler, J. W. Holmes and D. Roach, "Room Temperature Fatigue of a C-Fiber SiC-Matrix Composite," *J. Am. Ceram. Soc.*, accepted.

7. J. W. Holmes, X. Wu, and V. Ramakrishnan, "High-Frequency Fatigue of Fiber-Reinforced Ceramics," submitted to *J. Am. Ceram. Soc.*

Conference Presentations

1. S. F. Shuler, J. W. Holmes and J. Morris, "Influence of Frequency on the Rate of Damage Accumulation in a C-Fiber SiC-Matrix Composite," presented at the 15th Annual Conference on Ceramics and Advanced Composites, Cocoa Beach, FL, (January, 1991).

2. C. Cho and J. W. Holmes, "Frictional Heating in Fiber-Reinforced Ceramic Matrix Composites," presented at the 15th Annual American Ceramic Society Conference, Cincinnati, OH (April 1990).

3. C. Cho and J. W. Holmes, "Influence of Fatigue Loading and Test Frequency on Interfacial Shear Stress in Fiber-Reinforced Composites," 16th Annual Conference and Exposition on Ceramics and Advanced Composites, Cocoa Beach, FL, (January,1992).

4. V. Ramishkrishan, J. W. Holmes and M. Comninou, "High-Frequency Fatigue of Fiber-Reinforced Ceramics," presented at the 16th Annual Conference and Exposition on Ceramics and Advanced Composites, Cocoa Beach, FL, (January, 1992).

5. L. Butkus*, J. W. Holmes and T. Nicholas, "Thermomechanical Fatigue of a SiC-Fiber Calcium Aluminosilicate Matrix Composite," presented at the 16th Annual Conference and Exposition on Ceramics and Advanced Composites, Cocoa Beach, FL, (January, 1992).

6. J. W. Holmes, "Fatigue of Ceramic Matrix Composites Ceramics," 15th Automotive Materials Conference: Tough Ceramics, March 17, 1992, Ann Arbor, MI.

Invited Talks

1. J. W. Holmes, "Fatigue of Fiber-Reinforced Ceramics," Detroit TMS meeting, February, 1991.

2. J. W. Holmes, "Role of the Fiber-Matrix Interface in Internal Heating of Fiber-Reinforced Ceramics," TMS Fall Meeting, Cincinnati, OH, October, 1991.

3. J. W. Holmes, "High Frequency Fatigue of Fiber-Reinforced Ceramics," TMS/FEMS Symposium on Fatigue of Advanced Materials, TMS Annual Meeting, Denver, CO, February 22-25, 1993.

---

*Captain, USAF (Capt. Butkus obtained his MS Degree under the supervision of Professor Holmes. The experimental portion of his research was conducted at WPAFB). Dr. Ted Nicholas at WPAFB co-advised the thesis. The results obtained from Butkus' research are being published as a Technical Report at WPAFB and are therefore not elaborated upon in this report. A copy of the TR will be sent to AFOSR).

III. High Frequency Fatigue Life Degradation of a Fiber-Reinforced Ceramic Matrix Composite

III.1 Introduction

To-date investigations of fatigue life and fatigue damage accumulation in fiber-reinforced ceramics have been conducted at loading frequencies below 50 Hz.[1-8] However, recent studies[9-13] have shown that significant internal heating can occur during the fatigue of fiber-reinforced ceramics, which may influence fatigue life. The temperature rise during high frequency fatigue can be very substantial. For example, a temperature rise of approximately 100 K has been measured during the fatigue of unidirectional Nicalon/calcium-aluminosilicate composites at a loading frequency of 75 Hz between stress limits of 240 and 10 MPa.[12] Moreover, it has been shown for Nicalon/calcium-aluminosilicate composites, that the frictional shear stress present along the fiber/matrix interface decreases as the fatigue loading frequency is increased (this decrease is caused by differential thermal expansion between the fiber and matrix).[14] It has been previously postulated that the change in frictional shear stress, as well as temperature-induced microstructural damage, could result in a frequency dependence of fatigue life.[12] The purpose of the present communication is to report on recent findings that provide clear evidence for a frequency dependence of fatigue life in Nicalon/calcium-aluminosilicate composites.

III.2 Experimental Procedure

Unidirectional, 16-ply Nicalon/calcium-aluminosilicate composites (hereafter referred to as $[0]_{16}$-Nicalon/CAS-II) were used in the investigation. The composites, which contained 40 vol.% fibers, were manufactured by hot-pressing at a temperature of approximately 1350°C. Edge-loaded tensile specimens were machined from the hot-pressed billets using diamond tooling. The fibers were parallel to the specimen loading axis. The specimen gage-length was 33 mm, with a gage-section width of 6.3 mm and thickness of 3.2 mm (further details of the specimen geometry can be found in Chapter VI). The broad faces of the specimens were not machined. To allow acetate-film replicas of surface cracking to be obtained, the edges (minor faces) of the specimens were polished

with diamond paste to a final finish of 0.1 μm. An optical micrograph showing the typical fiber distribution in the test specimens is given in Fig. 1.

All fatigue experiments were conducted on a high resonant frequency servohydraulic load frame. The load-frame was equipped with a 6.8 kN actuator and edge-loaded grips. Because of the small force capacity of the actuator, monotonic tension tests were conducted on a higher-capacity load-frame equipped with a similar gripping arrangement. An isothermal test chamber, which surrounded the specimen and grips, was used to maintain the ambient temperature surrounding the specimens at 20 ±0.1C. The test chamber had a volume of 0.1 m^3. The temperature rise of the specimens was continuously measured throughout the fatigue experiments. For this purpose, optical pyrometers focussed at the center of the gage section were utilized.[1] The pyrometers had a spot size at the specimen surface of 5 mm. Further details concerning the experimental approach can be found in Reference 12.

Specimens were subjected to continuous fatigue loading at sinusoidal frequencies of 25, 75, 150 and 350 Hz. All experiments were conducted under load control (i.e., the maximum and minimum load limits, rather than displacement, were controlled). Specimens were fatigued at maximum stresses of 180, 200, 220 and 240 MPa; in all cases the minimum cyclic stress was held constant at 10 MPa. In practice, because of minor control problems, the lower fatigue limit fluctuated between 5 and 12 MPa. The upper fatigue limit was controlled to within 5 MPa. For the stress limits examined, the stress ratio ($\sigma_{min}/\sigma_{max}$) ranged from approximately 0.055 at 180 MPa to 0.041 at 220 MPa. Fatigue run out was defined as 5×10^6 cycles (this corresponds to approximately 55.5 h of testing at 25 Hz and 4 h of testing at 350 Hz). In addition to providing conventional stress *versus* cycles to failure data (i.e., an "SN" curve), this series of experiments provided information concerning the dependence of frictional heating on peak fatigue stress and loading frequency.

Information concerning the evolution of matrix crack spacing was determined for only two of

[1] Everest Interscience, Fullerton California. Pyrometer Model No. 5402 (for temperatures< 100°C); Pyrometer Model No. 5430 (for temperatures > 100°C). The two pyrometers were focussed on opposing sides of the specimen.

the fatigue loading histories: 25 and 75 Hz under a maximum stress of 180 MPa (since the process of obtaining replicas interferes with the measurement of temperature rise, which was one of the primary goals of the present study, crack spacings were not obtained for higher loading frequencies or stress levels). To avoid time-dependent matrix cracking during the taking of surface replicas, which can significantly influence the subsequent cycle dependence of crack spacing and modulus, all replicas were obtained with specimens loaded to a stress of 10 MPa. For comparison, the crack spacing was also determined for static loading at a maximum stress of 180 MPa (for this loading history the specimen stress was maintained at 180 MPa while obtaining the replicas). The values reported for matrix crack spacing were obtained from measurements made on a minimum of 500 crack-pairs (in many instances the cracks did not traverse across the entire specimen, but rather appeared to start and stop in a random fashion).

III.3 Results and Discussion

(1) Monotonic Tensile Behavior

The room-temperature monotonic tensile behavior of the composite is shown in Fig. 2. The composite exhibited a linear stress-strain response to a stress of approximately 285 MPa (defined as the proportional limit stress), followed by progressive nonlinear behavior. The failure strength of the composite was approximately 590 MPa. The initial tangent modulus was 131 GPa.

(2) Influence of Loading Frequency on Fatigue Life

The fatigue life of the composite is shown in Fig. 3 as a function of maximum fatigue stress and loading frequency. At a maximum fatigue stress of 180 MPa, fatigue run out was observed at all loading frequencies. Although there was scatter in the data at 150 and 350 Hz, it is clear for stresses above 180 MPa that the fatigue life decreased as the loading frequency was increased. For example, at 220 MPa the fatigue life was less than 300,000 cycles at frequencies of 150 and 350 Hz; this compares with over 5×10^6 cycles at 25 and 75 Hz. If time dependent (delayed crack growth) were the governing failure mechanism, the failure time would be independent of loading frequency. Plotting the failure time of specimens for the various loading histories, shows that this is clearly not the case; for stress levels above 200 MPa the failure time decreased with increasing

loading frequency.

It is very important to note that the fatigue experiments were conducted at stress levels (180 to 240 MPa) that were significantly below the monotonic proportional limit stress of virgin specimens (≈ 285 MPa). From the results of numerous investigations[1-7] it has been generally accepted that the proportional limit stress provides a rough approximation of the fatigue limit for many unidirectional fiber-reinforced ceramics fatigue (where the fatigue limit is defined as the stress level below which fatigue failures do not occur). All of these earlier investigations were conducted at loading frequencies of 10 Hz and lower (the 50 Hz fatigue experiments conducted by Shuler et al[8] were performed with C_f/SiC composites which do not exhibit a proportional limit stress because of processing related microcracking). However, the results obtained from the present investigation clearly suggest that the proportional limit stress cannot be used to predict the fatigue limit of fiber-reinforced ceramics at high loading frequencies. These results do not invalidate the use of the proportional limit stress as a predictor of the fatigue limit at lower loading frequencies (≤ 10 Hz), since the damage mechanisms at low loading frequencies will be different (i.e., will not be significantly influenced by internal heating).

(2) Frictional Heating During Fatigue Loading

As discussed in detail elsewhere[10-12], the repeated frictional slip of fibers along debonded interfacial slip-zones causes heat generation during the fatigue loading of fiber-reinforced ceramics. The frequency dependence of temperature rise is plotted in Fig. 4 for a maximum fatigue stress of 220 MPa. Figure 5 shows the influence of peak fatigue stress on temperature rise for a loading frequency of 350 Hz. As both of these figures indicate, the surface temperature rise can be quite substantial. For example, the temperature rise exceeded 160 K during 350 Hz fatigue at a peak stress of 240 MPa. As discussed below, frictional heating is thought to play a significant role in the reduced fatigue life found at high loading frequencies.

(3) Mechanisms Responsible for the Frequency Dependence of Fatigue Life

There is clear evidence from the present investigation that the rate and extent of microstructural

damage is frequency dependent. Figure 6 shows the change in matrix crack spacing that occurred during static loading at 180 MPa, and during fatigue at loading frequencies of 25 and 75 Hz (σ_{max} = 180 MPa). At a loading frequency of 25 Hz, the microcrack density stabilized within approximately 25,000 cycles, and remained constant thereafter. However, at a frequency of 75 Hz, the microcrack density continuously increased for the duration of the fatigue test (crack spacings at 150 and 350 Hz were not determined). There are similarities as well as important differences in the trends observed between the present study and an earlier study[12] of frictional heating and matrix damage in $[0]_{16}$ Nicalon/CAS-II composites. In the earlier study, which used a Nicalon/CAS-II composite with 5% fewer fibers, specimens were sequentially fatigued from 25 to 75 Hz. In agreement with measurements made in the present study, at 25 Hz there was an initial decay for the first 25,000 cycles, followed by a plateau in crack spacing (as expected for a reduced fiber fraction, the average crack spacing was also smaller than that measured in the present study). The equilibrium crack spacing that developed during initial fatigue at 25 Hz did not change during subsequent fatigue at 50 or 75 Hz. In contrast, in the present study, continuous 75 Hz fatigue caused a progressive increase in crack density. This increase at 75 Hz appears to be related to the damage state that develops in the initial stages of fatigue loading; in other words, the initial loading history of the composite determines subsequent crack growth behavior (this is one reason why it is important to state the precise procedure used to obtain surface replicas). Further investigations are in progress to determine the sensitivity of crack spacing to initial loading history.

At this time, the precise mechanisms which cause the frequency dependence of fatigue life and matrix damage are not known. It is likely that the reduction is related to the temperature rise during cyclic loading. Internal heating could influence the damage accumulation process by several mechanisms: (1) differential thermal expansion between the fiber and matrix can change the level of interfacial shear stress in the composite, resulting in a change in the distribution of load carried by the matrix and fibers, (2) the rate of interfacial wear could depend upon loading frequency, and (3) at high loading frequencies, where the temperature rise is large, heat transfer from the specimen surface may be rate limiting, resulting in very high internal temperatures within a fatigue specimen (this temperature rise could accelerate the rate of interfacial and microstructural damage). Using

microscopy to identify microstructural damage, and analytical modelling of the temperature distribution in the vicinity of the fiber-matrix interface, we are attempting to elucidate the mechanisms responsible for the frequency dependence of fatigue life. The results of these investigations will be reported in a future paper.

III.4 Conclusions

Based upon the results obtained from room temperature experiments conducted with unidirectional 16-ply Nicalon/CAS-II composites with 40 vol.% fibers, the following observations can be made regarding the influence of loading frequency on fatigue life:

1. Fatigue life decreases at high loading frequencies. At a peak stress of 220 MPa, the fatigue life decreased from 5×10^6 cycles (run out) at frequencies of 25 to 75 Hz, to less than 300,000 cycles at frequencies of 150 Hz and higher.

2. The proportional limit stress cannot be used as a predictor of fatigue limit at high loading frequencies. Failures occurred at maximum fatigue stresses that were significantly below the monotonic proportional limit stress. For example, at 350 Hz, failure was observed at a peak fatigue stress of 200 MPa (roughly 30% below the proportional limit stress and 66% below the ultimate strength). At 25 Hz, which was the lowest frequency examined, failures were observed at 240 MPa (approximately 15% below the proportional limit stress).

3. Microstructural damage increases at high loading frequencies. Although the crack spacing reached a plateau during static loading at 180 MPa and with fatigue loading at 25 Hz (σ_{max} = 180 MPa), the crack spacing showed a continual decrease during fatigue at 75 Hz under the same peak stress. This result is consistent with the observed reduction in fatigue life at the higher loading frequencies.

References

1. E. Minford and K. M. Prewo, "Fatigue of Silicon Carbide Reinforced Lithiumalumino-Silicate Glass-Ceramics," in Tailoring Multiphase and Composite Ceramics, C. G. Patano and R. E. Messing, Eds., Plenum Publishing Corporation, New York, 1986, pp. 561-70.

2. K. M. Prewo, "Fatigue and Stress Rupture of Silicon Carbide Fibre-Reinforced Glass-Ceramics," *J. Mater. Sci.*, **22** 2695-2701 (1987).

3. K. M. Prewo, "Tension and Flexural Strength of Silicon Carbide Fibre-Reinforced Glass-Ceramics," *J. Mater. Sci.*,**21** 3590-3600 (1986).

4. C. Q. Rousseou, "Monotonic and Cyclic Behavior of a Silicon Carbide/Calcium-Aluminosilicate Ceramic Composites," in Thermal and Mechanical Behavior of Metal Matrix and Ceramic Matrix Composites, ASTM STP 1080, J. M. Kennedy, H. H. Moeller, and W. S. Johnson (eds.), American Society for Testing and Materials, Philadelphia, PA, 1990.

5. L. P. Zawada, L. M. Butkus, and G. A. Hartman, "Room Temperature Tensile and Fatigue Properties of Silicon Carbide Fiber-Reinforced Aluminosilicate Glass," *Ceram. Eng. Sci. Proc.*, **11** [9-10] pp. 1592-1606 (1990).

6. L. M. Butkus and L. P. Zawada, "Room Temperature Tensile and Fatigue Properties of Silicon-Carbide Fiber-Reinforced Ceramic Matrix Composites," presented at Aeromat '90, Long Beach, CA, May 21-24, 1990.

7. P. G. Karandikar and T-W Chou, "Microcracking and Elastic Moduli Reductions in Unidirectional Nicalon-CAS Composites under Cyclic Loading," *Ceram. Eng. Sci. Proc.*, **13** [9-10] 881-888 (1992).

8. S. F. Shuler, J. W. Holmes and D.Roach, "Influence of Loading Frequency on the Rate of Damage Accumulation in a C-Fiber SiC-Matrix Composite," presented at the 15th Annual Conference on Ceramics and Advanced Composites, Cocoa Beach, FL, (January, 1991), Paper No. 116-C-91F. Submitted to *J. Am. Ceram. Soc.*

9. J. W. Holmes and S. F. Shuler, "Temperature Rise During Fatigue of Fibre-Reinforced Ceramics," *J. Mater. Sci. Lett.*, **9** 1290 - 1291 (1990).

10. C. Cho, J. W. Holmes and J. R. Barber, "Estimation of Interfacial Shear in Ceramic Composites from Frictional Heating Measurements," *J. Am. Ceram. Soc.*, **74** [11] 2802-2808 (1991).

11. J. W. Holmes and C. Cho, "Frictional Heating in a Unidirectional Fiber-Reinforced Ceramic Composite," *J. Mat. Sci. Lett.*, **11** (1992) 41-44.

12. J. W. Holmes and C. Cho, "Experimental Observations of Frictional Heating in a Fiber Reinforced Ceramics," *J. Am. Ceram. Soc.*, **75** [4] 929-38 (1992).

13. J. W. Holmes, "Fatigue of Fiber Reinforced Ceramics," Ceramics and Ceramic Matrix Composites, S. R. Levine (ed.), Vol. 3 in Flight-Vehicle Materials, Structures and Dynamics - Assessment and Future Directions, ASME, New York, 1992.

14. C. Cho and J. W. Holmes, "Influence of Fatigue Loading and Test Frequency on Interfacial Shear Stress in Fiber-Reinforced Composites," presented at the 16th Annual Conference and Exposition on Ceramics and Advanced Composites, Cocoa Beach, FL, (January,1992).

15. Personal communication, Ron Stewart, Corning Glass Works, Corning New York, December 1991.

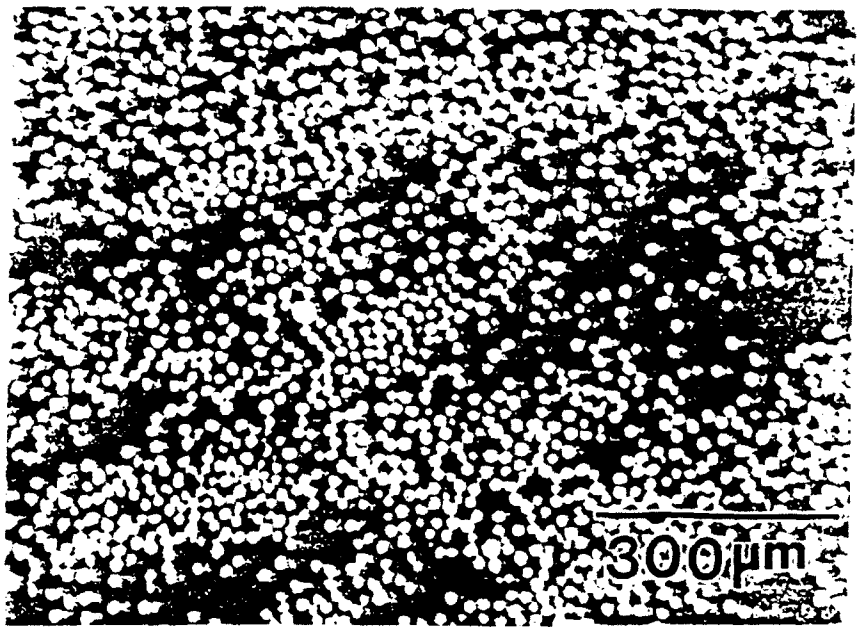

Fig. 1. Optical micrograph showing the typical fiber-distribution in the $[0]_{16}$-Nicalon/CAS-II specimens. The mean fiber diameter was 15.1 µm with a standard deviation of 2.5 µm.

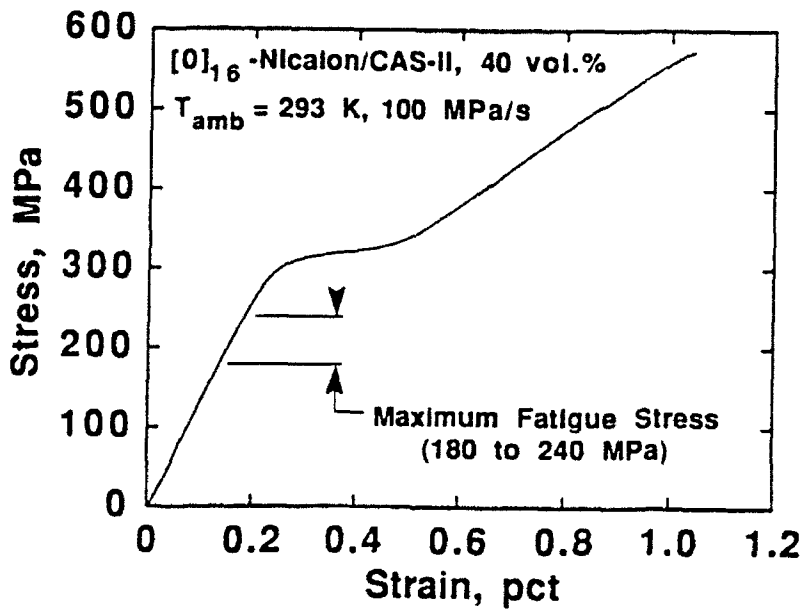

Fig. 2. Room temperature monotonic tensile behavior of 40 vol. % $[0]_{16}$-Nicalon/CAS-II. Specimens were loaded at a rate of 100 MPa/s to minimize the influence of time-dependent matrix cracking on the measured stress strain behavior. The proportional limit stress was approximately 285 MPa and the initial tangent modulus was 131 GPa. The maximum fatigue stresses used in the experiments are shown for comparison with the proportional limit stress and ultimate strength.

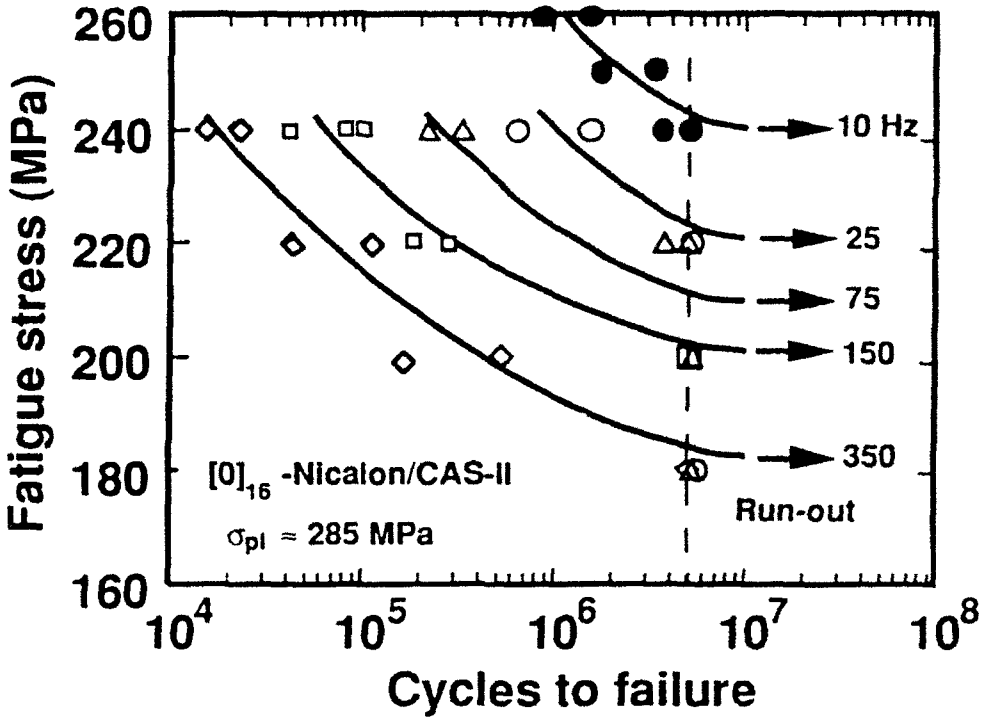

Fig. 3. Influence of maximum fatigue stress and sinusoidal loading frequency on fatigue life. For all experiments the minimum fatigue stress was 10 MPa and the ambient temperature was 293 K. At 180 MPa fatigue run out was observed for all loading frequencies.

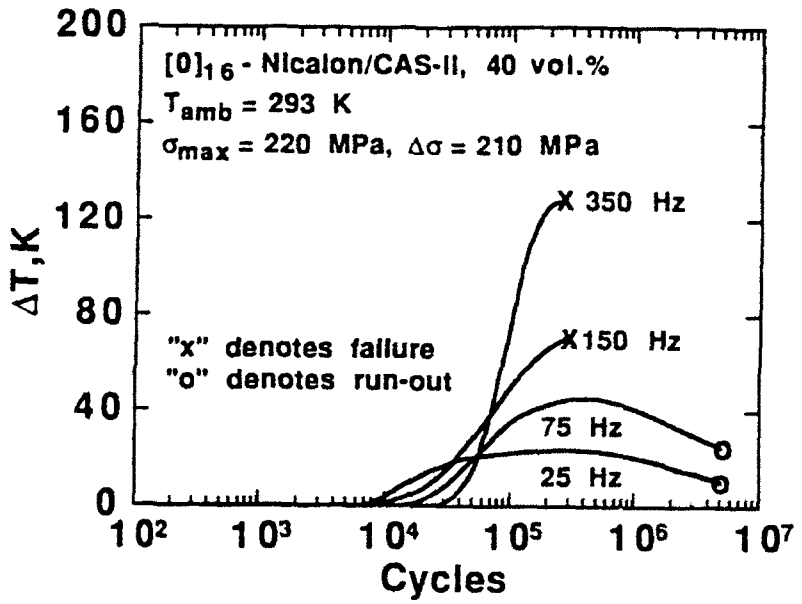

Fig. 4. Influence of loading frequency on the temperature rise ($T - T_{ambient}$) of $[0]_{16}$-Nicalon/CAS-II composites fatigued at a maximum stress of 220 MPa.

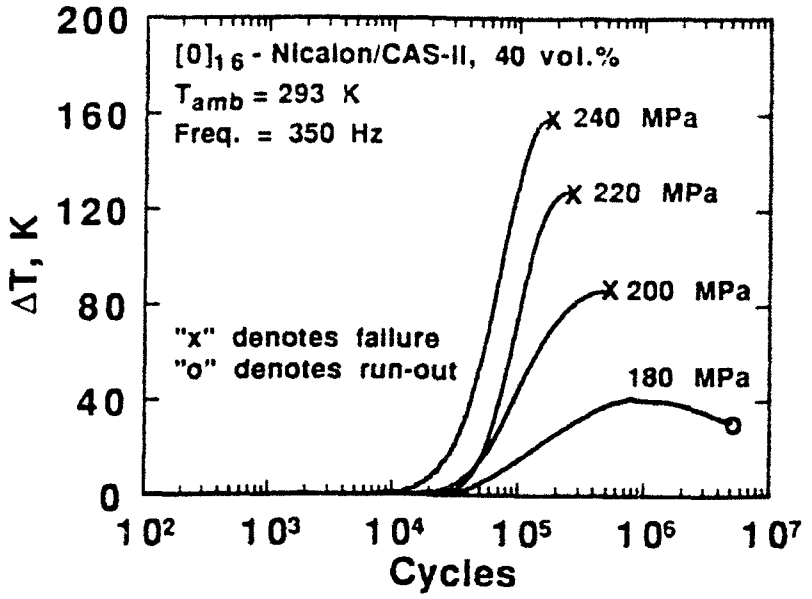

Fig. 5. Influence of maximum fatigue stress on the temperature rise ($T - T_{ambient}$) of $[0]_{16}$-Nicalon/CAS-II composites fatigued at a sinusoidal loading frequency of 350 Hz.

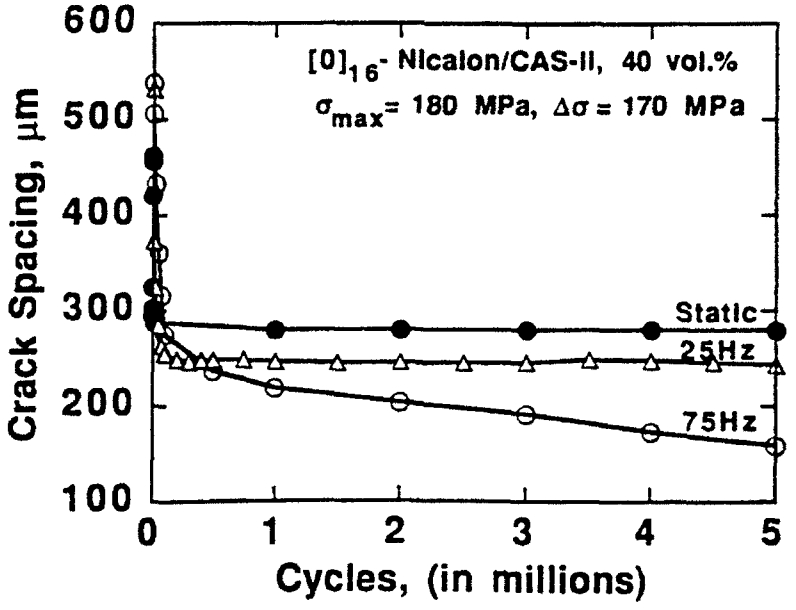

Fig. 6. Comparison of matrix crack spacing for fatigue loading at 25 and 75 Hz at a maximum fatigue stress of 180 MPa. For comparison, the crack spacing measured under static loading at 180 MPa is shown. At 25 Hz the crack spacing stabilized within approximately 25,000 cycles. Note that the crack spacing did not stabilize at 75 Hz.

IV. A New Approach for Estimation of Frictional Shear Stress in Fiber-Reinforced Ceramics

IV.1 Introduction

There are currently several approaches used to determine the frictional shear stress which exists along the fiber/matrix interface in fiber-reinforced ceramics. For example, Marshall [1,2] developed a straightforward indentation technique (fiber pushout) that has gained widespread acceptance and has been used to determine the interfacial shear stress in polymeric-matrix, metal-matrix and ceramic-matrix composites. A related approach, fiber-pullout [3,4], has also been widely used to measure interfacial shear stress. Both fiber pushout and fiber pullout experiments provide information regarding the interfacial shear stress which would exist under monotonic loading conditions. To compliment this information, there is a need to develop procedures which can be used to determine the interfacial shear stress which is present during fatigue loading.

Recent experiments by Holmes *et al* [5-7] indicate that significant internal heating can occur during the cyclic loading of fiber-reinforced ceramics. For example, a temperature rise of approximately 100 K was observed during the room temperature fatigue of unidirectional SiC-fiber calcium-aluminosilicate matrix composites at a frequency of 75 Hz and stress limits of 220 MPa and 10 MPa [7]. The temperature rise which occurs during cyclic loading, as well as cyclic wear damage along the fiber/matrix interface [8], could lead to differences in the interfacial shear stress which exists under monotonic and cyclic loading conditions.[2] The primary mechanism of internal heating in fiber-reinforced ceramics involves the frictional slip of fibers along debonded fiber/matrix interfaces [6]. For a frictional slip mechanism, the magnitude of internal heating would be related to the average frictional shear stress which exists along the fiber/matrix interface. Thus, by equating the work performed in the frictional sliding of fibers to the heat energy dissipated by a fatigue specimen, it should be possible to estimate the average level of frictional shear stress present along the fiber/matrix interface; the development of this approach forms the basis of the present communication.

[2]Under cyclic loading, differential thermal expansion between the fiber and matrix could lead to a frequency dependence of frictional shear stress (note that the degree of differential thermal expansion is determined by the thermal expansion mismatch between the fiber and matrix and the temperature rise which occurs during fatigue - the temperature rise is strongly influenced by both loading frequency and applied stress range [5,7]).

IV.2 Analysis

Work performed in the frictional slip of fibers

It is assumed that the cyclic frictional sliding of unfractured fibers within debonded interfacial slip-zones is the primary mechanism of internal heating which occurs in fiber-reinforced ceramics. The distance over which interfacial slip occurs during cyclic loading is controlled by the magnitude of the external load and the direction of loading [2,10,11]; thus, the active slip-length changes throughout a fatigue cycle. Depending upon the loading history, temperature, and composite system, fibers can undergo either partial slip, or a combination of partial and full frictional slip.[3] Thus for generality, two cases must be considered when determining the work performed in the frictional sliding of fibers: (I) partial frictional slip and, (II) partial/full frictional slip. In the analysis which follows, the slip-zone formed during loading will be referred to as a *forward* slip-zone; the slip-zone formed during unloading is referred to as a *reverse* slip-zone.

Case I: Partial frictional slip. For purposes of discussion, it is assumed that a composite has been subjected to the loading history shown in Fig. 1. A specimen is first loaded from zero stress to a stress $\sigma_{max'}$ along path OA'. During this initial loading, matrix cracking and interfacial debonding occur - this leads to the formation of a forward slip-zone of length $l_{fwd'}$ (Fig. 2). For path OA', the length of the forward slip-zone is equal to the distance over which debonding occurs. Neglecting elastic deformation outside the slip-zones, the fiber debond length δ can be estimated using an equation similar to that given by Thouless and Evans [12] for monotonic loading. At the maximum fatigue stress, $\sigma_{max'}$, forward slip-zone length is[4]

$$l_{fwd'}(\sigma_{max'}) = \delta = \frac{Cd_f\sigma_{max'}}{4\tau_d} \qquad (1)$$

[3]Partial slip refers to the situation where the active interfacial slip-length is always less than one-half of the matrix crack spacing. Full slip occurs when the active slip length equals one-half of the matrix crack spacing.

[4]Note that the expression given by Thouless and Evans [12] for slip-length is given terms of the fiber stress; whereas, Eq. 1 is expressed in terms of the far-field stress.

where, τ_d is the dynamic shear stress (frictional) along the fiber/matrix interface[5], d_f is the fiber diameter, and C is given in terms of the volume fraction of fibers (v_f) and the tensile moduli of the matrix and composite (E_m and E_c, respectively):

$$C = \frac{(1-v_f)E_m}{v_f E_c} \tag{2}$$

Upon stress reversal at point A', the loading path A'A is followed to the minimum cycle stress $\sigma_{min'}$. After achieving a stable crack density characteristic of fatigue at a maximum stress $\sigma_{max'}$, subsequent fatigue cycles are assumed to occur along path BB' ($\sigma_{max} \leq \sigma_{max'}$). The first loading path OA'A was included for generality since it determines the residual stress state which exists during subsequent loading at lower peak stresses. The instantaneous slip-zone length $l_{fwd}(\sigma)$ formed during loading from σ_{min} to σ can be found by graphical analysis of the matrix stress distribution shown in Fig. 3:

$$l_{fwd}(\sigma) = \frac{Cd_f}{8\tau_d}(\sigma - \sigma_{min}), \qquad \sigma_{min} \leq \sigma \leq \sigma_{max} \tag{3}$$

Outside the slip-zones, there is no relative displacement between the fiber and matrix; these regions of "stick" do not enter into the calculations for frictional work. The changes in fiber and matrix stress along the interface which occur during the loading portion of the fatigue cycle, can be determined by graphical analysis of the residual (prior) and current stress states shown in Fig. 3. For a change in stress from σ_{min} to σ, the stress increments can be expressed as follows:

$$\delta\sigma_f(z) = \frac{E_f}{E_c}(\sigma - \sigma_{min}) + \frac{8\tau_d z}{d_f}, \qquad 0 < z < l_{fwd} \tag{4}$$

$$\delta\sigma_m(z) = \frac{E_m}{E_c}(\sigma - \sigma_{min})\left(1 - \frac{z}{l_{fwd}}\right), \quad 0 < z < l_{fwd} \tag{5}$$

The corresponding increments in fiber and matrix displacement along the interface (denoted by δl_m and δl_f, respectively) can be obtained by integration of the stress increments:

[5]The terminology "dynamic shear stress" is used to emphasize that the frictional shear stress which is measured under cyclic loading conditions may differ from that measured using fiber pushout or pullout experiments.

$$\delta l_f(z) = \frac{(\sigma-\sigma_{min})z}{E_c} + \frac{4\tau_d z^2}{d_f E_f} \tag{6}$$

$$\delta l_m(z) = \frac{(\sigma - \sigma_{min})}{E_c}\left(z - \frac{z^2}{2l_{fwd}}\right) \tag{7}$$

The *relative* incremental displacement between the fiber and matrix, δl_{slide}, is given by the difference between the fiber and matrix displacements (Eqs. 6 and 7):

$$\delta l_{slide}(z) = \delta l_f(z) - \delta l_m(z) = \frac{4\tau_d z^2}{C d_f v_f E_f} \tag{8}$$

(note that Eq. 3 was substituted for l_{fwd} when simplifying Eq. 8). The increment in frictional work performed during loading is given by the incremental sliding distance (δl_{slide}) multiplied by the frictional force ($\pi d_f \tau_d dz$). Using an approach similar to that discussed by Thouless [13] for monotonic loading, the frictional work performed du ng loading from σ_{min} to σ_{max} can be determined by integrating over the active slip length:

$$W_{load} = 2\int_0^{l_{fwd}(\sigma)} \delta l_{slide}(z)\,[\pi d_f \tau_d]dz = \frac{\pi d_f^3 C^2 \Delta\sigma^3}{(3)(64) v_f E_f \tau_d} \tag{9}$$

where, $\Delta\sigma = \sigma_{max} - \sigma_{min}$, and the factor of two is used to account for symmetry of the interfacial slip-zones (see Fig. 2).

Upon unloading from σ_{max} to σ, a reversed slip-zone of length $l_{rev}(\sigma)$ develops:

$$l_{rev}(\sigma) = \frac{C d_f}{8\tau_d}(\sigma_{max} - \sigma), \qquad \sigma_{min} \le \sigma \le \sigma_{max} \tag{10}$$

The frictional work performed during unloading can be shown to be equal to that for loading (this can be shown using an analysis similar to that used to derive Eq. 9). Thus the total work performed in one complete loading-unloading cycle becomes:

$$W_{total} = 2W_{load} = 2\left(\frac{\pi d_f^3 C^2 \Delta\sigma^3}{(3)(64)v_f E_f \tau_d}\right) = \frac{\pi d_f^3 C^2 \Delta\sigma^3}{96 v_f E_f \tau_d} \tag{11}$$

Dividing Eq. 11 by the unit cell volume, $\pi d_f^2 \bar{l}/4v_f$ (see Fig. 2), and multiplying by the loading frequency f, gives the total frictional energy dissipation per unit volume:

$$\frac{dw_{fric}}{dt} = \frac{f C^2 d_f \Delta\sigma^3}{24 E_f \bar{l} \tau_d} \tag{12}$$

Note that the above analysis holds even if full frictional slip occurs during initial loading to $\sigma_{max'}$ (path OA'); the only requirement is that full slip does not occur during subsequent loading between σ_{max} and $\sigma_{min'}$ (path BB'). The case where both partial and full frictional slip occur within the same fatigue cycle is analyzed below.

Case II: Partial/full frictional slip. As with case I (partial frictional slip), the specimen is first loaded from zero stress to a stress $\sigma_{max'}$ (path OA'). If $\sigma_{max'}$ is of sufficient magnitude, the interfacial slip-zones will become saturated at an intermediate level of stress denoted by σ_{slip} (i.e., at σ_{slip}, interfacial slip occurs over a distance equal to the mean crack spacing $\bar{l}$). During initial loading along path OA', the applied stress level at which full frictional slip begins is determined by the interfacial shear stress and mean crack spacing $\bar{l}$:

$$\sigma_{slip} = \frac{2\tau_d \bar{l}}{C d_f} \tag{13}$$

Upon unloading from $\sigma_{max'}$ to an intermediate stress σ, full frictional slip will begin when the change in stress equals $2\sigma_{slip}$. After unloading to σ_{min} (path A'B), the residual stress-state shown in Fig. 4 will exist. Reloading from σ_{min} to an intermediate stress σ gives rise to a forward slip-zone of length $l_{fwd}(\sigma)$ (see Fig. 4):

$$l_{fwd}(\sigma) = \frac{C d_f}{8\tau_d}(\sigma - \sigma_{min}) \tag{14}$$

If the stress range during subsequent loading to σ_{max} exceeds $2\sigma_{slip}$, full frictional slip occurs. As the stress is increased beyond that necessary to initiate full slip, the *additional* increment in external load is supported only by the fibers. To determine the work performed in the frictional slip of fibers, the loading path must be divided into two regimes: (i) a partial slip regime which occurs for $\sigma_{min} < \sigma < \sigma_{min} + 2\sigma_{slip}$ and, (ii) a full slip regime which occurs for $\sigma_{min} + 2\sigma_{slip} < \sigma < \sigma_{max}$. Since the work performed during loading and unloading are equal, only the work performed during loading is considered in the analysis which follows.

(i) Partial slip: $\sigma_{min} < \sigma < \sigma_{min} + 2\sigma_{slip}$. Within this interval, the analysis is similar to case I. The changes in fiber and matrix stress along the interface which occur during the loading portion of the fatigue cycle can be determined by graphical analysis of the residual (prior) and current stress states shown in Fig. 4. As with case I (Eq. 9), the stress increments can be used to determine the *relative* incremental displacement between the fiber and matrix, δl_{slide}, which can then be integrated to determine an expression for the frictional work performed during loading:

$$W_{load} = \frac{\pi d_f^3 C^2 (2\sigma_{slip})^3}{(3)(64) v_f E_f \tau} \tag{15}$$

(ii) Full slip: $\sigma_{min} + 2\sigma_{slip} < \sigma < \sigma_{max}$. In this interval, the forward slip length, l_{fwd}, equals one-half of the mean crack spacing, $\bar{l}$. As noted above, once full frictional slip occurs, the additional load is supported entirely by the fibers; no further change in matrix stress occurs. The incremental changes in axial stress in the fiber and matrix which occur during loading are:

$$\delta\sigma_m(z) = 0 \tag{16}$$

$$\delta\sigma_f(z) = \frac{\sigma_{max} - (\sigma_{min} + 2\sigma_{slip})}{v_f} = \frac{\Delta\sigma - 2\sigma_{slip}}{v_f} \tag{17}$$

Since only the fibers undergo additional loading, the strain increment $(\delta\sigma_f(z)/E_f)$ is constant within a slip-zone. When this condition is reached, the relative incremental displacement between the fiber and matrix at a distance z from the edge of the slip-zone, $\delta l_{slide}(z)$, equals the

increment in fiber displacement, $\delta l_f(z)$:

$$\delta l_{slide}(z) = \delta l_f(z) = \frac{(\Delta\sigma - 2\sigma_{slip})z}{v_f E_f} \tag{18}$$

Within the range $\sigma_{min} + 2\sigma_{slip} < \sigma < \sigma_{max}$, the frictional work performed during loading to σ_{max} can be obtained by integrating Eq. 18 over the active slip length (*i.e.*- from $z = 0$ to $z = \bar{l}/2$):

$$W_{load} = 2\int_0^{\frac{\bar{l}}{2}} \delta l_{slide}(z)[\pi d_f \tau_d]dz = \left(\frac{\pi d_f^2 \bar{l}}{4v_f}\right)\left(\frac{\bar{l}\tau_d}{d_f}\right)\left(\frac{\Delta\sigma - 2\sigma_{slip}}{E_f}\right) \tag{19}$$

Adding Eqs. 15 and 19, the total frictional work performed during loading from σ_{min} to σ_{max} can be expressed as

$$W_{load} = \frac{\pi d_f^2 \bar{l}}{4v_f}\left(\frac{d_f C^2 (2\sigma_{slip})^3}{(3)(16)E_f \bar{l}\tau_d} + \left(\frac{\bar{l}\tau_d}{d_f}\right)\left(\frac{\Delta\sigma - 2\sigma_{slip}}{E_f}\right)\right) \tag{20}$$

As noted earlier, the frictional work performed during loading and unloading are equal; thus, $W_{total} = 2W_{load}$. Substituting $4\tau_d\bar{l}/Cd_f$ for $2\sigma_{slip}$ in Eq. 20, dividing by the unit cell volume, and multiplying by the loading frequency f, gives the total frictional work rate when both partial and full frictional slip occur within a fatigue cycle:

$$\frac{dw_{fric}}{dt} = \frac{2f\bar{l}\tau_d\Delta\sigma}{d_f E_f} - \frac{16f\tau_d^2\bar{l}^2}{3E_f C d_f^2} \tag{21}$$

Calculation of heat loss during fatigue

Assuming a steady-state microstructural damage state and temperature rise has been attained in a composite during cyclic loading, and neglecting other modes of energy dissipation, the heat loss from the composite to isothermal surroundings must equal the work performed in the frictional slip of fibers. For a fatigue specimen, such as that shown in Fig. 5, convective and radiative heat losses ($[dq/dt]_{conv}$ and $[dq/dt]_{rad}$, respectively) will occur from the specimen

surface (the surface area is denoted by A_{surf}). Additional heat loss by conduction ($[dq/dt]_{cond}$) will occur through a cross-section which is perpendicular to the fibers (denoted by A_{cond}). The total rate of heat loss per unit volume, dq/dt, is given in terms of the surface temperature of the specimen T_s, air temperature T_a, convective heat transfer coefficient h, emissivity ε, and the thermal conductivity of the composite parallel to the fibers k:[6]

$$\frac{dq}{dt} = \left[\frac{dq}{dt}\right]_{conv} + \left[\frac{dq}{dt}\right]_{rad} + \left[\frac{dq}{dt}\right]_{cond}$$

$$= \left[h(T_s - T_a) + \varepsilon\beta(T_s^4 - T_a^4)\right]\frac{A_{surf}}{V} + \frac{2kA_{cond}}{V}\left[\frac{\Delta T}{\Delta z}\right]_{axial} \qquad (22)$$

where, β is the Stefan-Boltzman constant (5.67×10^{-8} W/m^{2}K^4), $[\Delta T/\Delta z]_{axial}$ is the axial temperature gradient at the end of gage-section and V is the gage-section volume. It is important to note that as an alternative to estimating dq/dt from Eq. 22 (which requires measurement of the temperature rise, $(T_s - T_a)$), the energy dissipation during cyclic loading can be estimated by calculating the area enclosed by a cyclic stress-strain (hysteresis) curve and multiplying by the loading frequency *f* (this also provides a means by which the accuracy of the heat loss analysis can be determined). Under steady-state conditions, the mechanical work performed in the frictional slip of fibers dw_{fric}/dt (Eq. 12 or 21) must equal the rate of heat loss to the surroundings dq/dt (Eq. 22). Thus equating dw_{fric}/dt to dq/dt (or alternatively equating dw_{fric}/dt to the energy dissipation calculated from cyclic stress-strain curves) provides an equation where the only unknown is the frictional shear, τ_d.

IV.3 Application of Model

To illustrate the application of the analysis discussed above, the frictional shear stress present in a unidirectional Nicalon™/CAS-II composite[7] will be estimated. The technique involves conducting tension-tension fatigue experiments and determining the rate of energy dissipation. Prior to conducting the fatigue experiments, it is important that a stable matrix crack spacing has been achieved; this is most easily accomplished by pre-fatiguing a specimen at a maximum stress

[6]For a general discussion of heat transfer the reader is referred to Holman [15].

[7]Composites manufactured by Corning Glass Works, Corning, NY. CAS-II is the Corning Glass Works designation for a calcium-aluminosilicate matrix.

which is equal to or greater than the peak stress used in the subsequent frictional heating experiments used to determine energy dissipation.

The 16-ply composite was processed with 35 vol. % fibers. Edge-loaded tensile specimens, with a 33 mm gage-length, were used in the fatigue experiments (Fig. 5). The experiments were performed in air using an isothermal test chamber which completely surrounded the specimen and grips [7]. The chamber was held at a temperature of 293 K ±0.1K; the relative humidity within the chamber was 65%. All fatigue experiments were conducted at a sinusoidal loading frequency of 25 Hz. The temperature rise at the specimen surface was measured using a high-resolution infrared pyrometer[8] which was focused at the center of the specimen gage-section. The cyclic stress-strain curves were also recorded to allow comparing the frictional energy dissipation with dq/dt (Eq. 22). Further details concerning the experimental procedure can be found in References 6 and 7.

To achieve a constant matrix crack spacing prior to measurement of the temperature rise, a specimen was first pre-fatigued for 100,000 cycles between fixed stress limits of 180 MPa and 10 MPa (Fig. 6a).[9] After approximately 20,000 cycles, the mean crack spacing approached a plateau at approximately 198 μm (the crack spacing was determined by periodically unloading the specimen and using surface replication with acetate film). Next, as illustrated in Fig. 6a, the specimen was subjected to cyclic loading at stress ranges of 90, 110 and 130 MPa. Several stress ranges were included to determine the sensitivity of the technique to peak stress and stress range and to provide confidence in the data trends. Since the amount of energy dissipation is influenced by matrix crack spacing, it is important that the maximum stress used in the pre-fatigue experiment is not exceeded. The steady-state temperature rise measured for each stress range is shown in Fig. 6b. Measurements of the average crack spacing, which were made after each constant stress-range experiment, showed that the crack spacing remained essentially constant at 198 μm.

Using the data given in Table I, and the temperature rise data given in Fig. 6b, the dynamic shear stress was determined for the two frictional work cases discussed above - *i.e.*, partial slip and partial/full frictional slip. Assuming partial frictional slip, and using Eqs. 12 and 22 for the

[8]Everest Interscience Inc., Fullerton, CA, USA. Model No. 5402.

[9]A peak stress below the proportional limit strength (225 MPa [6]) was chosen to minimize fiber fracture.

energy balance, τ_d would be between 3.5 MPa to 4.5 MPa for the three stress ranges examined (see Fig. 7). Assuming partial/full frictional slip occurs during fatigue, and using Eqs. 21 and 22, τ_d would be approximately 0.4 MPa for all stress ranges. Experiments conducted on two additional specimens gave essentially the same values for frictional shear stress (the values differed by less than 5%). As mentioned above, as an alternative to calculating the rate of heat loss from Eq. 22, the energy dissipation can be determined from the cyclic stress-strain curves and equated directly to Eqs. 12 or 21. Using this approach provided results which were similar to those obtained by using the heat loss equation (the comparison for the case of partial frictional slip is shown in Fig. 7).

To determine which analysis (*i.e.*, partial slip or partial/full slip) was applicable for the temperature and loading conditions which were examined, the experimentally measured cyclic stress-strain curves (Fig. 8a) were compared with those predicted using the values of frictional shear stress calculated above. To calculate the cyclic stress-strain curves, the stress and strain distribution in the fiber was estimated for the cases of partial slip and partial/full slip (a graphical approach similar to that shown in Figs. 3 and 4 was used to determine the stress-strain curves).[10] Figure 8b, shows the calculated cyclic stress-strain curves for the partial slip assumption. Although the predicted modulus was much higher than the experimentally measured modulus, the dependence of average modulus on stress range showed a similar trend (*i.e.*, in both instances, the average modulus decreased as the maximum fatigue stress was increased)[11]. This trend is consistent with partial slip behavior. Assuming partial/full slip occurs during the fatigue cycle ($\tau_d = 0.4$), the average modulus would remain constant as the maximum fatigue stress is increased - this result is *not consistent* with the experimentally observed trend shown in Fig. 8a. For the case of partial slip, the discrepancy between the calculated modulus and the experimentally measured modulus is thought to arise from fiber fracture which occurred during the initial fatigue experiments which were conducted between stress limits of 10 MPa and 180 MPa (note that fiber fracture was not included when determining the theoretical stress-strain curves). Although fiber fracture was not included in the analysis of frictional energy dissipation,

[10]From the axial stress distribution in the fiber, the axial strain in the slip-zones is found directly through integration of the displacement. Within the regions bridged by fibers, the additional strain resulting from fiber loading is given by $\sigma/v_f E_f$.

[11]The decrease in modulus is caused by the increase in the slip-zone length which occurs as the applied stress is increased.

the total number of fractured fibers would be small for the loading histories examined. Thus, since the majority of interfacial slip-zones would still be populated by unfractured fibers, the error introduced in the calculation of shear stress by neglecting the slip of fractured fibers is expected to be small.

From the discussion presented above, the partial slip analysis is appropriate for determining the interfacial shear stress present in the specific composite and loading conditions used in the frictional heating experiments -from Fig. 7, the dynamic shear stress is between approximately 3.5 to 4.5 MPa. Wang and Parvizi-Majidi [17] have measured the frictional shear stress in Nicalon™/CAS-II composites; the shear stress ranged from 12.4±2.6 for fiber pushout experiments, to 17.7±2.6 MPa for fiber push-in experiments. These values correspond to the frictional shear stress which would be present in virgin material immediately after interfacial debonding. Under cyclic loading, however, the repeated frictional sliding of fibers (either fractured or unfractured) can produce wear damage along the fiber-matrix interface. Thus the relatively low value of frictional shear stress (3.5 to 4.5 MPa) which was found in the present paper is most likely a consequence of interfacial wear damage that occurred during the fatigue experiments. Evidence for a reduction in frictional shear stress caused by the fatigue loading of composite materials has been obtained from fiber pushout experiments conducted by Mackin *et al* [8] on Ti-vanadium composites. Singh and Sutcu [18] have also observed a decrease in frictional shear during repeated fiber pushout/pushback experiments conducted with SiC/zircon composites.

IV.4 Summary

A new technique for estimating the interfacial shear stress present during the cyclic loading of fiber-reinforced ceramics has been developed. To generalize the model, it will be necessary to include the influence of fractured fibers on the frictional energy dissipation which occurs during fatigue; this will require knowledge of the statistical distribution of fiber strength and the failure location of fibers. A potential advantage of the frictional heating technique for determining interfacial shear stress is that an average value of frictional shear stress is obtained, rather than a value based upon discrete measurements made on individual fiber/matrix interfaces. The technique can also be readily extended to allow determining the temperature dependence of

interfacial shear stress. Also, since the temperature rise can be determined on a continuous basis, it is possible to continuously monitor the change in frictional shear stress which occurs during cyclic loading [7]; this may be a useful approach for determining the influence of fiber coatings on the rate of interfacial wear. A limitation of the proposed frictional heating technique is that it can only provide information concerning the frictional shear stress which exists during cyclic loading. Other well established approaches, such as fiber-pushout [1,2] and fiber pull-out experiments [3,4], are required to determine the shear required to initiate debonding, and the frictional shear stress which is present immediately after the debonding of virgin interfaces.

IV.5 References

1. D. B. Marshall, "An Indentation Method for Measuring Matrix-Fiber Frictional Stresses in Fiber-Reinforced Ceramic Composites," *J. Am. Ceram. Soc.*, **67** [12] C-259 - C-260 (1984).

2. D. B. Marshall and W. C. Oliver, "Measurement of Interfacial Mechanical Properties in Fiber-Reinforced Ceramic Composites," *J. Am. Ceram. Soc.*, **70** [8] 542-548 (1987).

3. K. T. Faber, S. H. Advani, J. K. Lee, and J. T. Jinn, "Frictional Stress Evaluation Along the Fiber-Matrix Interface in Ceramic Matrix Composites," *J. Am. Ceram. Soc.*, **69** [9] C-208 - C-209 (1986).

4. R. W. Goettler and K. T. Faber, "Interfacial Shear Stresses in SiC Alumina Fiber Reinforced Glasses," *Ceram. Eng. Sci. Proc.*, **9** [7-8] 861-872 (1988).

5. J. W. Holmes and S. F. Shuler, "Temperature Rise During Fatigue of Fibre-Reinforced Ceramics," *J. Mater. Sci. Lett.*, [9] 1290 - 1291 (1990).

6. J. W. Holmes and C. Cho, "Frictional Heating in a Fiber-Reinforced Ceramic Composite," *J. Mater. Sci. Lett.*, in press.

7. J. W. Holmes and C. Cho, "Experimental Investigation of Frictional Heating in Fiber-Reinforced Ceramics," *J. Am. Ceram. Soc.*, submitted.

8. T. J. Mackin, P. D. Warren and A. G. Evans, "Fiber Pushout of a Fatigued Specimen," presented at the 93rd Annual ACS Meeting, Cincinnati, OH, April 28 - May 2, 1991, Paper No. 54-SVI-91.

9. C. Cho, J. W. Holmes and J. R. Barber, "Distribution of Matrix Cracks in a Uniaxial Ceramic Composite", *J. Am. Ceram. Soc.*, submitted.

10. R. M. McMeeking and A. G. Evans, "Matrix Fatigue Cracking in Fiber Composite", *Mechanics of Materials*, **9** 217 - 227 (1990).

11. B. N. Cox, "Interfacial Sliding near a Fibrous or Layered Composite During Thermal Cycling", *Acta. Metall. Mater.*, **38** [12] 2411 - 2424 (1990).

12. M. D. Thouless and A. G. Evans, "Effects of Pull-Out on The Mechanical Properties of Ceramic Matrix Composites," *Acta Metall.*, **36** [3] 517 - 522 (1988).

13. M. D. Thouless, "A Re-examination of The Analysis of Toughening in Brittle-Matrix Composites," *Acta Metall.*, **37** [9] 2297 - 2304 (1989).

14. R. A. [illegible], and H. T. Hahn, "Effect of Interfacial Properties on Matrix Cracking Stress in Fiber Reinforced Ceramics," in Symposium on High Temperature Composites, Technomic Publishing Co., Lancaster, PA, 148 - 157 (1989).

15. J. P. Holman, Heat Transfer, McGraw-Hill Inc., 346 (1986).

16. Information sheet on Nicalon™ fibers and calcium-aluminosilicate provided by Corning Glass Works, Corning, NY (1991).

17. S. W. Wang and A. Parvizi-Majidi, "Mechanical Behavior of Nicalon™ Fiber-Reinforced Calcium-Aluminosilicate Matrix Composites," *Ceram. Eng. Sci. Proc.*, **11** [9-10] 1607 - 1616 (1990).

18. R. N. Singh and M. Sutcu, "Determination of Fiber-Matrix Interfacial Properties in Ceramic Matrix Composites by a Fiber Push out Technique," *J. Mater. Sci.*, in press (1991).

Table I. Data used to estimate τ_d for a unidirectional 16-ply Nicalon™/CAS-II composite.

Parameter	Comments
A_{surf} (surface area of specimen gage section) = 662.6 mm^2	Fig. 5
A_{cond} (cross-sectional area of specimen gage section) = 23.3 mm^2	"
E_f (tensile modulus of fiber) = 200 GPa	Ref. 14
E_m (tensile modulus of matrix) = 88 GPa	"
f (loading frequency used in fatigue experiments) = 25 Hz	—
h (free convection heat transfer coefficient)	Ref. 15*
k (thermal conductivity of composite parallel to the fibers) = 5.16 W/m-K	Ref. 16
$\bar{l}$ (mean crack spacing) =198 μm	from microscopy
v_f (fiber volume fraction) = 0.35	"
ΔT (steady-state temperature rise)	Fig. 6b
$[\Delta T/\Delta z]_{axial}$ (average axial temperature gradient from edge of gage-section to grips)	---
V (gage section volume) = 768.9 mm^3	Fig. 5
ε (surface emissivity of composite) = 1.0	assumed value

* $h = 1.42\left(\frac{T_s - T_a}{L}\right)^{\frac{1}{4}}$ [units: W/m^2-K]. L refers to the gage-section length.

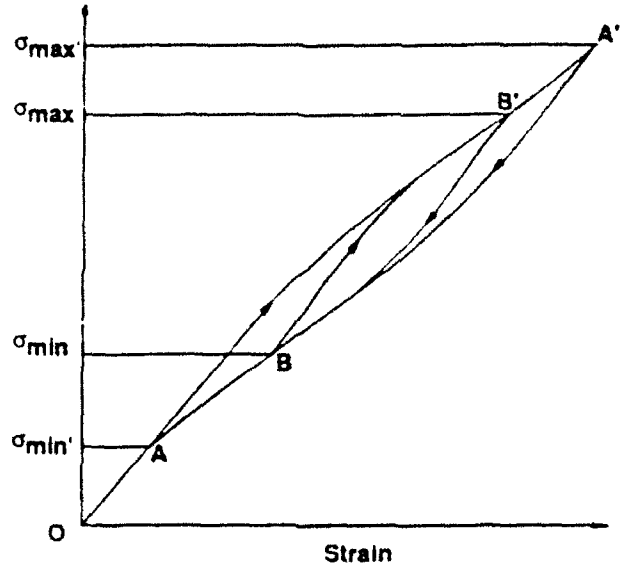

Fig. 1. Loading path used to calculate the frictional energy dissipation in fiber-reinforced ceramics subjected to cyclic loading. Consistent with the experiments used to obtain a stable crack density prior to temperature rise measurements, initial fatigue is assumed to occur between stress limits of $\sigma_{max'}$ and $\sigma_{min'}$ (path AA'). Subsequent fatigue cycles occur at a lower stress range, between stress limits of σ_{max} and σ_{min} (path BB').

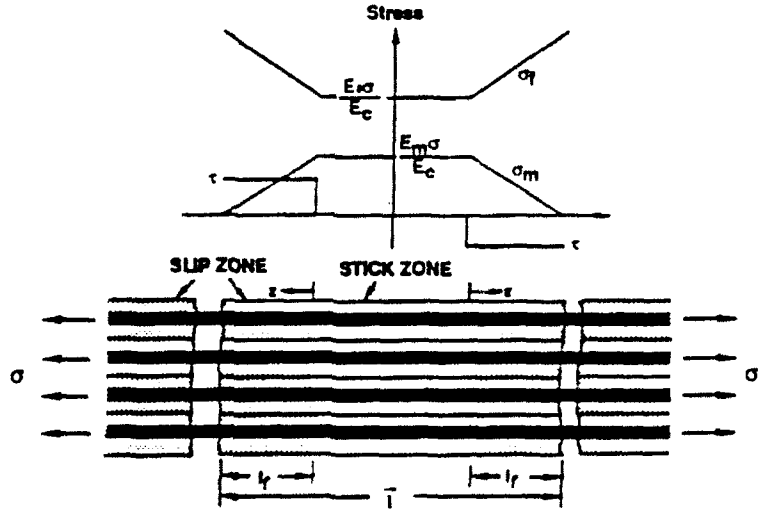

Fig. 2. Axial stress distribution in the matrix and fiber during initial monotonic loading from zero-stress to an intermediate stress level σ. As a simplification, the shear stress is assumed to be constant within the interfacial slip-zones of length l_f (an exact solution for the stress distribution can be found in Reference [7]). The unit cell has a length equal to the experimentally determined mean crack spacing $\bar{l}$.

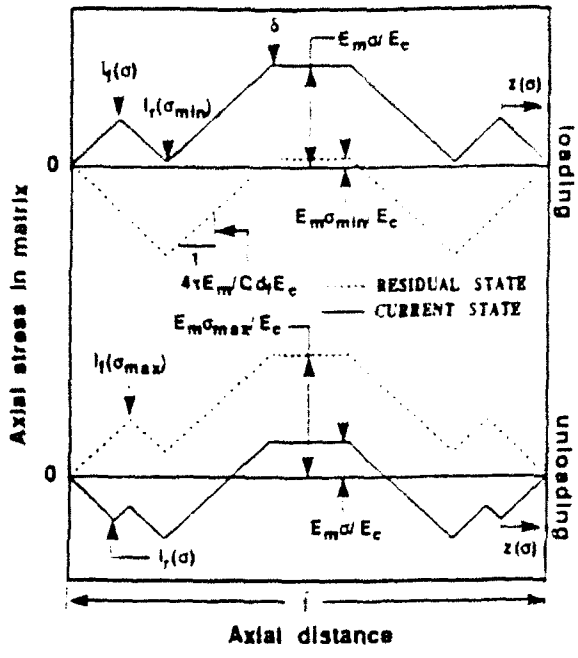

Fig. 3. Stress distribution in the matrix during loading and unloading for the case of partial slip. Loading is assumed to occur from σ_{min} to an intermediate stress σ. Unloading occurs from σ_{max} to σ.

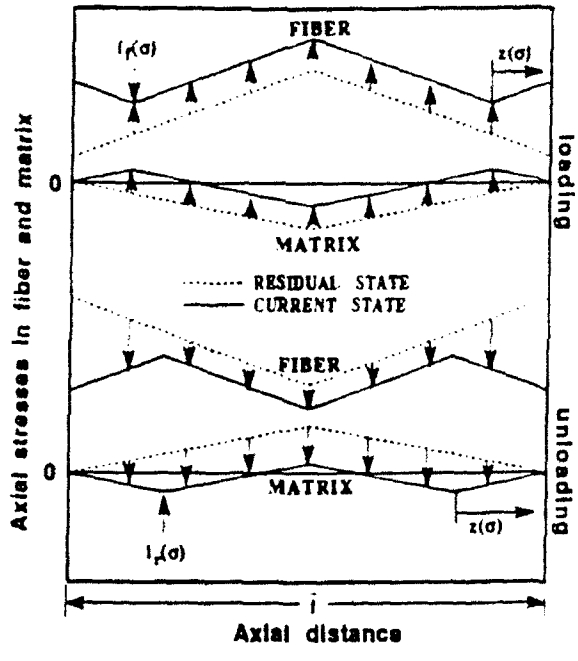

Fig. 4. Stress distribution in the fiber and matrix during loading and unloading for the case of full frictional slip. The composite is loaded or unloaded to an intermediate stress σ. During the initial stage of loading and unloading partial slip occurs; for this stage of loading only those regions where $z \geq 0$ contribute to the frictional work. At higher stress levels, full frictional slip occurs throughout the interfacial slip zones (in this instance, $z = \bar{l}/2$).

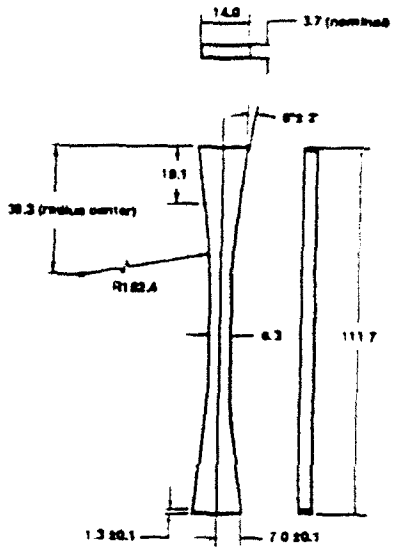

Fig. 5. Edge-loaded specimen used in the fatigue experiments. The specimen had a gage-length of 33 mm. Other specimen geometries and gripping arrangements can be utilized so long as a large volume of uniformly stressed material is present (e.g., face-loaded rectangular specimens). Dimensions in millimeters.

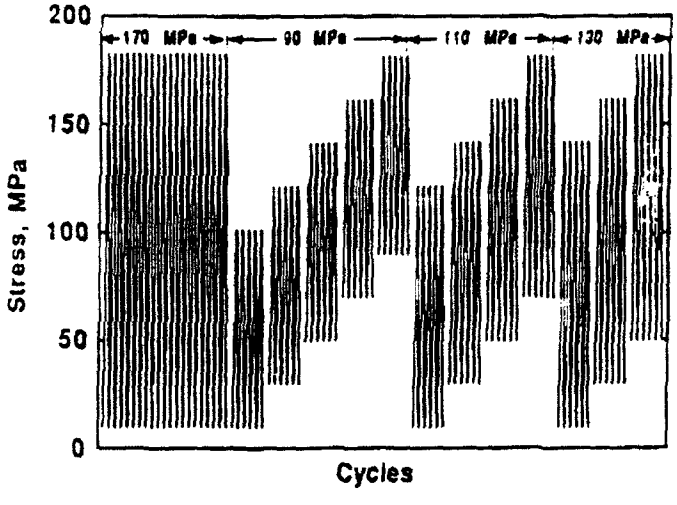

(a)

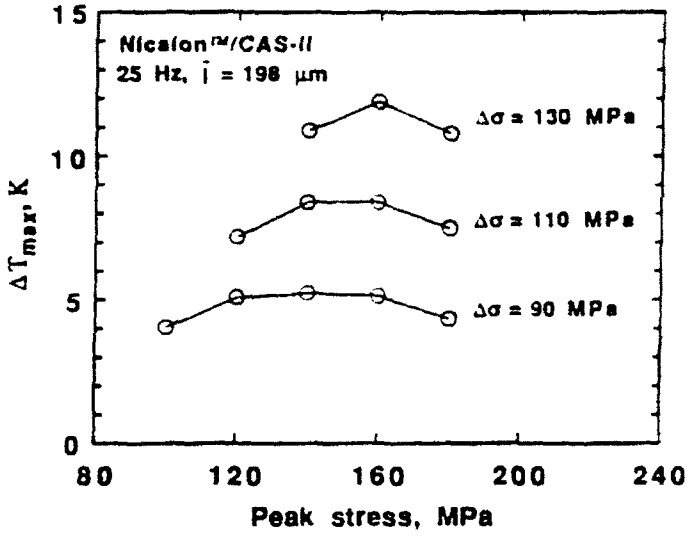

(b)

Figs. 6a and b. (a) Loading history used to determine the influence of stress-range on temperature rise. To achieve a stable crack density, the specimen was initially fatigued between stress limits of 180 MPa and 10 MPa. Subsequent fatigue experiments were conducted for 25,000 cycles each. All experiments were conducted at a loading frequency of 25 Hz. The stress range (in MPa) is given above each group of stress-cycle curves. (b) Temperature rise versus stress range for unidirectional Nicalon™/CAS-II. The initial temperature of the composite was 293 K.

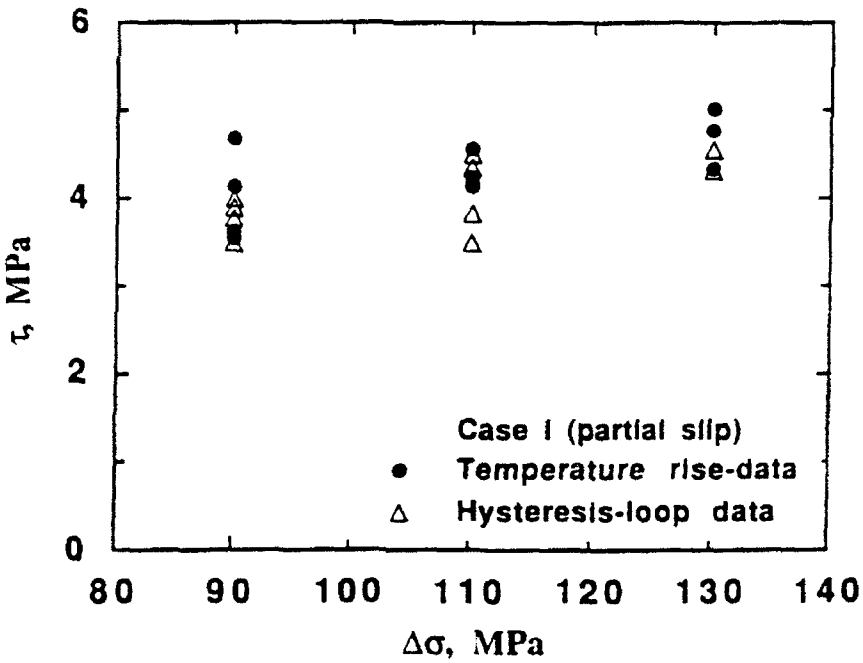

Fig. 7. Dynamic frictional shear stress, τ_d, estimated from Eq. 12. The shear stress was determined for a loading frequency of 25 Hz For comparison, both temperature rise data and the cyclic stress-strain (hysteresis) curves were used to determine the frictional energy dissipation. Both approaches provide similar results.

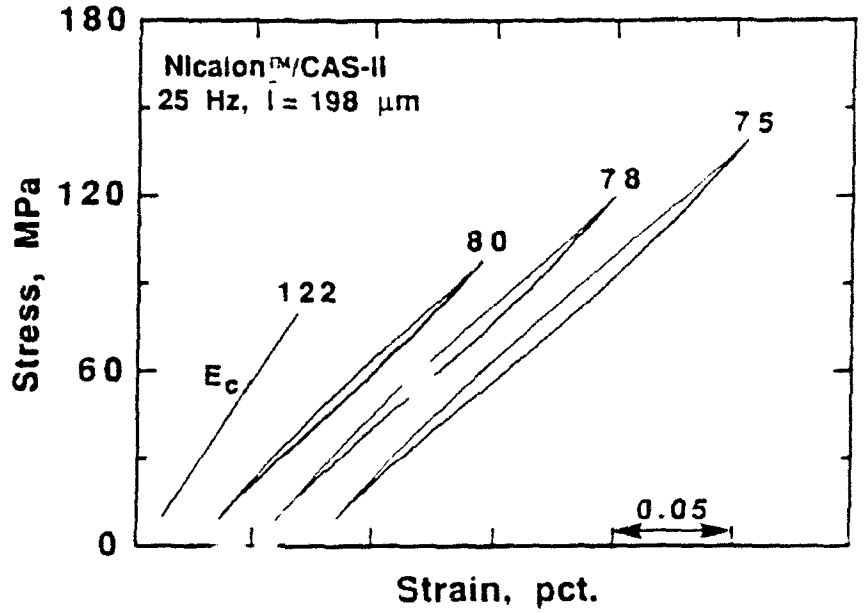

(a)

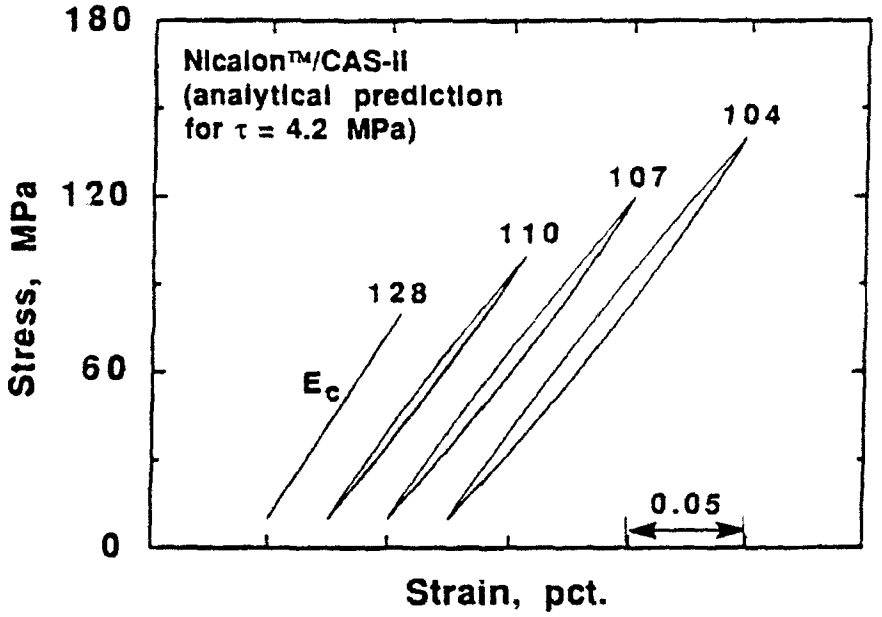

(b)

Figs. 8a and b. Hysteresis curves formed during the cyclic loading of unidirectional Nicalon™/CAS-II. (a) Experimentally measured. (b) Analytical prediction for the case of partial frictional slip. The average modulus for the fatigue cycle is shown above each curve (units: GPa).

V. Influence of Fatigue Loading History and Matrix Damage on Frictional Heating in Fiber-Reinforced Ceramics

V.1 Introduction

During cyclic loading, considerable hysteresis in the stress-strain response of fiber-reinforced ceramics is commonly observed at ambient and elevated temperatures.[1-5] This hysteresis, which is a measure of the energy dissipation during a fatigue cycle, is related to the frictional slip of fibers along debonded interfacial slip-zones.[6-9] The repeated frictional sliding of fibers can give rise to very substantial internal heating during the cyclic loading of fiber-reinforced ceramics.[5,10,11] For example, a temperature rise of 30 K was observed during the room temperature fatigue of cross-ply C_f/SiC composites at 85 Hz between stress limits of 250 MPa and 10 MPa.[10] A more dramatic temperature rise of 50 K has been measured during the fatigue of unidirectional SiC-fiber/calcium-aluminosilicate matrix composites at 25 Hz between stress limits of 240 MPa and 10 MPa.[11]

The occurrence of frictional heating in ceramic matrix composites is of both practical and fundamental significance. From a practical viewpoint, fiber-reinforced ceramics are under development for use in advanced gas-turbines, heat exchangers and space-based structures. For these applications, a temperature rise caused by frictional heating could result in unacceptable dimensional changes, as well as changes in the mechanical behavior and thermophysical properties of the composite. From a fundamental viewpoint, the temperature increase which occurs during fatigue could alter the interfacial shear stress in a composite (through differential thermal expansion between the fiber and matrix), leading to a frequency dependence of mechanical behavior, including toughness, strength, modulus, fatigue life and

mechanical damping. It is also possible that differential thermal expansion between the fiber and matrix could cause the further extension of initial interfacial debonding. As a consequence of the low thermal conductivity of many ceramic matrices, the local temperature rise in the vicinity of the fiber-matrix interface may be significantly higher than the bulk temperature rise. Independent of the operating temperature of a component or structure, a further temperature increase at the interface (by frictional heating) could result in an increased rate of chemical diffusion near the fiber/matrix interface. For applications where energy dissipation is desired, frictional heating could be an asset, since it provides a potent mechanism for the dissipation of mechanical energy during monotonic and cyclic loading.

The present paper builds upon an earlier experimental investigation of frictional heating in SiC-fiber/calcium-aluminosilicate composites (hereafter referred to as Nicalon/CAS-II)[f12] which established a correlation between the initiation of matrix cracking and the onset of frictional heating.[11] Specifically, this paper examines the relationship between stress range, loading frequency and matrix crack spacing on the magnitude of frictional heating and the change in interfacial shear stress which occurs during the fatigue of Nicalon/CAS-II composites.

V.2 Experimental Procedure

Material, specimen geometry and test method. A 16-ply unidirectional Nicalon/CAS-II calcium-aluminosilicate matrix composite was used in this investigation. The composite,

[f12]Composites processed by Corning Inc., Corning, NY, USA. Nicalon is the designation for SiC-fibers produced by Nippon Carbon, Tokyo Japan. CAS-II is the Corning designation for the calcium aluminosilicate matrix used in this composite system.

formed by hot-pressing into rectangular billets, had a nominal fiber content of 35 vol. %. Edge-loaded tensile specimens with a 33 mm gage-length (see Fig. 1) were machined from the billet using diamond tooling. Specimens were removed from the billet such that the reinforcing fibers were parallel to the tensile loading axis. An optical micrograph showing the typical fiber distribution in the specimens is shown in Fig. 2. The minor faces of the specimen gage-section were polished with diamond paste to an 0.1 μm finish to allow acetate-film replicas of surface cracking to be obtained.

Monotonic tension and tension-tension fatigue testing was conducted on an MTS Model 810 servohydraulic load-frame[f13] equipped with edge-loaded grips. Details of the gripping arrangement and typical bending strains have been discussed elsewhere.[12] A water-cooled test chamber, which completely surrounded the specimen and grips (see Fig. 3), was used to maintain the air temperature in the vicinity of the specimen at 293 ±0.1 K. The relative humidity within the chamber was between 65% and 67%. Gage-section strains were measured using a clip-on extensometer.[f14] The extensometer was mounted along one of the specimen edges (Fig. 3). Extensometer and load-cell signals were gathered using a high-speed 16-bit resolution data acquisition system.[f15] During the fatigue experiments, the specimen temperature was measured with an infrared pyrometer which was focused at the center of the specimen gage-section to a diameter of 5 mm.[f16] The pyrometer had a resolution (background noise level) of 0.1 K and a response time of 300 ms. The pyrometer

[f13]MTS Systems Corporation, Minneapolis, MN, USA.

[f14]MTS Systems Corporation, Minneapolis, MN, USA. Model No. 632.27B-20; modified for a 33 mm gage length.

[f15]GW Instruments, Sommerville, MA, USA. Model MBC-625 with 16-bit 50 kHz daughterboards.

[f16]Everest Interscience Inc., Fullerton, CA, USA. Model No. 5402.

data was collected by a separate 16-bit resolution data acquisition system.[f17] The temperature within the isothermal test chamber was allowed to equilibrate for 5 h prior to starting the fatigue experiments. Monotonic tensile tests and the initial loading ramps used in the fatigue experiments were conducted at a constant loading rate of 100 MPa/s. A rapid loading rate was used to prevent time-dependent matrix cracking.[f18] All fatigue experiments were performed under load-control using a sinusoidal waveform.

The fatigue tests were periodically interrupted to obtain surface replicas of matrix crack spacing; a stress of 10 MPa was maintained on the specimen while taking the replicas. Although crack definition could be improved slightly by increasing the tensile stress at which the replicas were taken, the use of a higher stress (e.g., 50 MPa) was found to cause time-dependent matrix cracking within the 5 minutes required to obtain a replica. Time dependent cracking was observed only during the initial stages of fatigue - prior to the establishment of a stable crack density. Surface replicas were obtained from only one of the specimen edges (the location of the extensometer prevented taking replicas along both edges). However, results obtained from several trial experiments conducted without the extensometer showed that the average crack spacing along the two edges typically differed by only 2 to 4 μm. Moreover, these trial experiments showed essentially identical results when measurements of crack spacing were made along the broad faces of the gage-section. To obtain confidence in the data trends, at least 140 crack pairs were measured. Using optical and scanning electron

[f17]Strawberry Tree Computers, Sunnyvale, CA, USA. Model No. ACM2-16

[f18]Time-dependent matrix cracking at room temperature can significantly influence the proportional limit stress, ultimate strength and overall shape of the monotonic stress-strain curve for fiber-reinforced ceramics. This effect is most apparent when loading rates below 10 MPa/s are used; for most ceramic composites, loading rates of 50 to 500 MPa/s give essentially identical stress-strain curves.

microscopy of the surface replicas, the average crack spacing could be confidently determined to within ±2.0 μm.

V.3 Results and Discussion

Tensile behavior. The monotonic tensile behavior of the Nicalon/CAS-II composite at 293 K is shown in Fig. 4. The initial deviation from linear behavior occurred at approximately 225 MPa; using notation introduced by Prewo and co-workers[2,3], this stress level will be referred to as the proportional limit strength, σ_{pl}. The proportional limit corresponds to the occurrence of a mechanically detectable amount of matrix or fiber damage. When defined in this manner, the value assigned to the proportional limit strength is influenced by the sensitivity of the extensometer and load cell, as well as the loading or displacement rate used during monotonic loading. As discussed below, during fatigue, matrix cracking was first observed at a peak stress of 120 MPa, which is approximately 50% below the monotonic proportional limit strength measured with virgin specimens.

Initiation of frictional heating. Although discussed in detail elsewhere[11], it is convenient to briefly review recent experimental results which showed that the onset of frictional heating during cyclic loading coincides with the initiation of matrix cracking. To establish this correlation, an experiment was conducted wherein the peak fatigue stress was increased in 20 MPa steps from 100 MPa to 260 MPa. During this experiment, which was conducted at a sinusoidal loading frequency of 25 Hz, the minimum fatigue stress was held constant at 10 MPa. The specimen was fatigued for 25,000 cycles at each peak stress. The initiation of matrix cracking, and subsequent change in crack spacing as the peak stress was increased, was determined by taking surface replicas after the first fatigue cycle and at the completion of

each 25,000 cycle fatigue loading block.

Based upon two test results, neither a temperature rise or matrix cracking were observed at 100 MPa. Coinciding with the formation of several matrix cracks, a temperature rise of 0.3 K to 0.4 K was measured at a peak fatigue stress of 120 MPa. As mentioned earlier, this stress is approximately 50% *below* the monotonic proportional limit strength of the composite. Noting that interfacial debonding and the formation of interfacial slip-zones typically accompanies matrix cracking, this result provided experimental confirmation that the frictional sliding of fibers is responsible for the internal heating which occurs in fiber-reinforced ceramics. The experiment was continued at higher peak stresses to investigate the relationship between maximum temperature rise, stress range and mean crack spacing. The temperature rise curves are shown in Fig. 5. As shown in Fig. 6, the average matrix crack spacing approached an approximate plateau between peak stresses of 200 MPa and 240 MPa. For a constant crack spacing, the roughly 25 K temperature rise between 200 MPa and 240 MPa is higher than the temperature rise which would be expected based solely on an increase in stress range (see later discussion). Thus, other factors, such as the occurrence of additional fiber fractures and an increase in the debond length of fibers, contribute to the temperature rise.

In the experiments described above, no attempt was made to separate the influence of peak fatigue stress, stress range and matrix crack spacing on the extent of frictional heating. The remainder of this paper discusses experiments which were performed in an attempt to isolate the effect of these variables. Whenever possible, the experimental trends were established using a single specimen; thus avoiding potential errors in the interpretation of the experimental

results that could arise from slight variations in fiber distribution and volume fraction between specimens.

Influence of stress range and peak fatigue stress on frictional heating. Trial experiments had shown that once a constant crack density was achieved at a given peak stress, fatigue at peak stresses equal to or below this stress would not alter the crack spacing. Thus, to determine the influence of peak fatigue stress and stress range on temperature rise at a fixed crack spacing, a series of constant stress range experiments were conducted using a specimen which was initially "prefatigued" for 100,000 cycles at 25 Hz between fixed stress limits of 180 MPa and 10 MPa. Next, an experiment was conducted wherein the stress range was held constant, while the peak fatigue stress was sequentially increased in 20 MPa steps up to the initial pre-fatigue stress of 180 MPa. Using the same specimen, this experiment was performed at stress ranges of 90, 110 and 130 MPa. The specimen was fatigued for 25,000 cycles for each combination of peak stress and stress-range. A schematic of the loading history is shown in Fig. 7.

During prefatigue at 180 MPa, the specimen was periodically unloaded to 10 MPa to allow measurement of the matrix crack spacing. From these measurements, the mean crack spacing approached a constant value of 198 μm within 20,000 cycles (see Fig. 8). After an initially rapid decay, the cyclic stress-strain modulus approached an approximate plateau within 50,000 cycles. The initial decrease in modulus is attributed to matrix cracking and interfacial debonding. The lag in stabilization of the cyclic stress-strain modulus, which occurred at a slower rate than stabilization of the crack spacing, is attributed to additional interfacial debonding which would continue to occur even after a constant crack spacing was achieved. A slight (<2%) recovery in modulus was observed between approximately 75,000 and

100,000 cycles; as discussed later, a further recovery in modulus occurs during longer duration fatigue experiments. A similar modulus recovery has been observed in unidirectional Nicalon/aluminosilicate composites[13], 3-D braided SiC_f/SiC[13] and 0°/90° C_f/SiC[5].

The matrix crack spacing was measured at the completion of each 25,000 cycle loading block used in the constant stress range experiments; the matrix crack spacing remained essentially constant at 198 μm (as mentioned earlier, the crack spacing remains constant so long as the pre-fatigue stress is not exceeded). As shown in Fig. 9a, the maximum temperature rise exhibited an approximately linear dependence on stress range; a 20 MPa increase in stress range resulted in an average temperature increase of 3.2 K. In contrast to the marked sensitivity to stress range, the temperature rise showed only a weak dependence on peak fatigue stress. For example, at a stress range of 90 MPa, the temperature rise varied by less than 1 K when the peak stress was increased by 80 MPa (see Fig. 9a). When the maximum temperature rise is plotted against total strain range (Fig. 9b), an approximately linear relationship is found. For a constant crack spacing, the frictional sliding distance of fibers, and hence the amount of heat energy generated, scales with the specimen strain range. Thus, the linear relationship between strain range and temperature rise is consistent with a mechanism of internal heating involving the repeated frictional sliding of fibers within debonded interfacial slip-zones.

Examination of Fig. 9b shows that for a given stress range the temperature rise reached a maximum at intermediate levels of peak stress. In Fig. 10, the hysteresis curves from the experiments conducted at a constant stress range of 130 MPa are plotted. Comparison of Fig. 9a and Fig. 10, shows that the peak in temperature rise corresponds to a peak in energy

dissipation at intermediate levels of peak fatigue stress. The mechanism responsible for this peak in energy dissipation is not known at this time. It is also interesting to note that the shape and area of the hysteresis envelope formed by merging the individual hysteresis curves obtained during the constant stress range experiments is approximately the same as the hysteresis curve obtained by fatiguing directly between the extremes of the stress limits used in the constant stress range experiments (in this case between 180 MPa and 10 MPa). Thus, once a constant crack density has been achieved at a given peak stress and stress range, say for example, after fatigue between 180 MPa and 10 MPa, the energy dissipation and temperature rise which would occur at lower peak stresses can be estimated from the 180 MPa/10 MPa hysteresis curves. This approach would drastically reduce the number of experiments required to characterize the history dependence of frictional heating which occurs for a given matrix crack spacing.

Influence of crack spacing and test frequency on internal heating. For a mechanism of internal heating involving the frictional slip of fibers along interfacial slip zones, the extent of internal heating will depend upon the total number and length of the debonded slip-zones which are present in the composite. The number of debonded zones is a function of the mean crack spacing[14-16], which, in turn, is determined by the maximum fatigue stress. Since the energy dissipation (as heat) depends upon the number of slip-zones, the temperature rise should increase as the mean crack spacing decreases. To investigate the relationship between matrix crack spacing and temperature rise, the crack spacing in a specimen was sequentially decreased by prefatiguing at maximum stresses of 160, 180, 200 and 220 MPa. Each pre-fatigue experiment was conducted for 50,000 cycles a loading frequency of 25 Hz and a minimum stress of 10 MPa. After prefatiguing at a given maximum stress (to achieve a stable

crack spacing characteristic of the particular stress level), the specimen was sequentially fatigued at frequencies of 5, 10, 25, 50 and 75 Hz between fixed stress limits of 160 MPa and 10 MPa (the loading history is shown in Fig. 11). At each loading frequency, the specimen was fatigued for 1000 s - which was sufficient for the temperature rise to attain an approximate plateau. After each 1000 s fatigue loading block, the specimen was allowed to cool to ambient temperature prior to fatiguing at the next loading frequency. The stress levels used in the pre-fatigue experiments provided average matrix crack spacings $\bar{l}$, which ranged from 228 μm at a peak stress of 160 MPa, to 181 μm at a peak stress of 220 MPa (see Fig. 12). The average crack spacing was also measured after each 1000 s fatigue loading block to determine if the initial crack spacing changed during the variable-frequency experiments; in all cases, there was no measurable change in crack spacing.

Typical temperature rise curves obtained during the variable-frequency fatigue experiments are shown in Fig. 13. The maximum temperature rise is plotted in Fig. 14a, as a function of mean crack spacing and loading frequency. At a given frequency the maximum temperature rise increased as the crack spacing decreased. This is to be expected; as the crack spacing decreases, the total number of interfacial slip zones present in the specimen increases, providing additional sites for heat generation by frictional slip. The inverse relationship between temperature rise and average crack spacing is consistent with a mechanism of internal heating involving the frictional sliding of fibers (as discussed in the next section, the area enclosed by the stress-strain hysteresis loops, which is proportional to the energy dissipation per cycle, also increases as the mean crack spacing is decreased). Although there was no appreciable difference in mean crack spacing for the pre-fatigue experiments conducted at peak stresses of 200 MPa and 220 MPa[f19], a higher temperature rise was observed after pre-

[f19]The mean crack spacing decreased from 184 μm to 181 μm. In view of the error in measuring crack

fatigue at 220 MPa (Fig. 14a). This further temperature rise is attributed to the additional debonding and fiber-fractures which would be present after pre-fatigue at 220 MPa.

After completion of the experiments described above, and using the same specimen, additional information regarding the stress-range and frequency dependence of frictional heating was obtained by comparing, at a crack spacing of 181 μm, the magnitude of the temperature rise which occurred at peak stresses of 160 MPa and 220 MPa (see Figure 14b). At a peak stress of 220 MPa the temperature rise was substantial; exceeding 100 K at a loading frequency of 75 Hz. Examination of surface replicas taken before and after the experiment conducted at 220 MPa showed no change in crack spacing.

Influence of long-duration fatigue on temperature rise. During the tension-tension fatigue of 0°/90° C_f/SiC composites produced by chemical vapor infiltration, Holmes and Shuler[10] observed an initial peak in specimen temperature, followed by a gradual decay. In parallel with the temperature decay, a slight increase in the average stress-strain modulus occurred. The initial decay in specimen temperature was postulated to be the result of a decrease in interfacial shear stress caused by wear damage along the fiber-matrix interface. To determine if a similar temperature decay occurs in unidirectional Nicalon/CAS-II composites, a virgin specimen was subjected to continuous 25 Hz fatigue between fixed stress limits of 180 MPa and 10 MPa. As shown in Figs. 15a and b, the temperature rise reached an initial peak within the first 30,000 cycles, followed by a sharp decrease of approximately 1 K and a gradual recovery in temperature which persisted until approximately 750,000 cycles.

---

spacing (±2 μm), this small difference is not considered experimentally significant.

Beyond 750,000 cycles the temperature rise slowly decayed. A sharp increase in temperature rise was observed immediately prior to specimen failure.

The changes in specimen temperature were roughly paralleled by changes which occur in the amount of stress-strain hysteresis. As shown in Fig. 16, the hysteresis slowly increases towards an initial maximum at approximately 50,000 cycles. For the stress limits and loading frequency used in the experiment, the crack spacing stabilized within approximately 20,000 cycles (see Fig. 8); thus, the additional strain ratchetting which occurred between 20,000 and 50,000 cycles is attributed to further interfacial debonding. Although further strain ratchetting occurred between 50,000 and 3.18×10^6 cycles, the extent of hysteresis decreased by less than 5%. A large increase in hysteresis occurred immediately prior to specimen failure, which occurred at approximately 3.21×10^6 cycles.

The average cyclic stress-strain modulus exhibited an initially rapid decay - from an initial value of 120 GPa to approximately 70 GPa after 30,000 fatigue cycles (Figs. 15a and b). This rapid modulus decay is attributed to the formation of matrix cracks and debonding along the fiber/matrix interface. Beyond approximately 100,000 cycles, the modulus slowly recovered; to roughly 80 MPa immediately prior to specimen failure. Under load-controlled fatigue, an increase in specimen modulus produces a proportional decrease in strain amplitude ($\Delta\sigma \propto E_c \Delta\varepsilon$). Noting that the amount of heating is qualitatively related to strain range (see Fig. 9b), the modulus recovery which occurred during cyclic loading appears to be partially responsible for the gradual decay in temperature observed beyond approximately 750,000 fatigue cycles. As discussed in a later section, the modulus recovery is attributed to a partial

recovery in frictional shear stress.

Comments on damping behavior and cyclic stress-strain behavior. For the experiments described in the preceding section, the maximum temperature rise showed an approximately linear dependence on loading frequency within the range of 5 Hz to 25 Hz. At higher frequencies, the temperature rise was significantly less than that predicted by a linear extrapolation of data obtained at frequencies of 25 Hz and lower. Two possible mechanisms for this trend are: (1) differential thermal expansion between the fiber and matrix causes a slight reduction in interfacial shear stress and (2) other modes of energy dissipation were present at frequencies of 50 Hz and higher. The first possibility is consistent with the thermal expansion mismatch between Nicalon fibers and the CAS matrix: $\alpha_{Nicalon} \approx 4 \times 10^{-6}\ °C^{-1}$ and $\alpha_{CAS} \approx 5 \times 10^{-6}\ °C^{-1}$.[17] Thus, for Nicalon/CAS-II composites, a bulk temperature rise would cause a decrease in normal stress and, therefore, shear stress across the interface. The later possibility is suggested by examination of Figs. 17a and b, which show that a significant change in the cyclic stress-strain behavior occurs at loading frequencies of 50 Hz and 75 Hz. Recent experiments conducted using a much stiffer loading frame with a resonant frequency above 300 Hz[f20], showed no appreciable distortion of the hysteresis loops when similar specimens were tested at frequencies up to 150 Hz. Thus, the change in stress-strain behavior at 50 and 75 Hz appears to be caused by compliance of the loading frame, rather than a change in the intrinsic damping behavior of the composite. These experiments also indicate that for a significant temperature rise by frictional heating, the interfacial shear stress decreases at loading frequencies above 50 Hz.[18]

[f20] An MTS Servohydraulic Model 331 load-frame was used in these experiments.[20]

Influence of loading frequency on interfacial (frictional) shear stress. Cho et al.[19] recently developed an approach whereby the frictional shear stress which is present during the cyclic loading of fiber-reinforced ceramics can be estimated by analysis of frictional heating data. The approach involves performing an energy balance to relate the energy dissipated through the frictional slip of fibers to the heat loss from a fatigue specimen to its surroundings. Assuming that the fibers undergo partial frictional slip, the work performed in the frictional slip of fibers dw_{fric}/dt, is given in terms of the loading frequency f, applied stress range $\Delta\sigma$, average matrix crack spacing $\bar{l}$, and dynamic frictional shear stress τ_d:

$$\frac{dw_{fric}}{dt} = \frac{f d_f \Delta\sigma^3}{24 E_f \bar{l} \tau_d}\left[\frac{(1-v_f)E_m}{v_f E_c}\right]^2 \qquad (1)$$

where, E_f, E_m and E_c are the initial tensile moduli of the fibers, matrix and composite, respectively and v_f and d_f are the fiber volume fraction and fiber diameter, respectively. Neglecting other modes of mechanical energy loss, the energy dissipated as frictional work, dw_{fric}/dt, equals the rate of heat loss to the surroundings. The rate of heat loss can be determined by summing the convective, radiative and conductive heat losses from the fatigue specimen.[f21] Alternatively, the heat loss can be obtained directly from the cyclic stress-

[f21] The rate of heat loss per unit volume, dq/dt, is given in terms of the surface temperature of the specimen T_s, air temperature T_a, convective heat transfer coefficient h, emissivity ε, and the thermal conductivity of the composite parallel to the fibers k:

$$\frac{dq}{dt} = \left[h(T_s - T_a) + \varepsilon\beta(T_s^4 - T_a^4)\right]\frac{A_{surf}}{V} + \frac{2kA_{cond}}{V}\left[\frac{\Delta T}{\Delta z}\right]_{axial}$$

where, β is the Stefan-Boltzman constant (5.67×10^{-8} W/m^2-K^4), $[\Delta T/\Delta z]_{axial}$ is the axial

strain hysteresis curves obtained during a fatigue test (the energy dissipation per cycle is determined by calculating the area enclosed by a cyclic stress-strain curve and multiplying by the loading frequency).

Using Equation 1, and the temperature rise data given in Fig. 14a, τ_d was determined as a function of loading frequency and mean crack spacing. As shown in Fig. 18, within the range of 5 to 25 Hz the interfacial shear is approximately constant. Higher frequency data was not considered since machine compliance caused distortion of the hysteresis curves at 50 and 75 Hz. The calculated interfacial shear stress shows a slight dependence on mean crack spacing, ranging from approximately 6 MPa at 228 μm, to 3 MPa at 184 μm and 181 μm. Noting that the crack spacing was changed by sequentially increasing the maximum fatigue stress, the apparent dependence of interfacial shear stress on crack spacing is most likely a consequence of additional microstructural damage which occurred during prefatigue at the higher peak stress levels. In particular, the extent of interfacial debonding and number fiber fractures would increase with an increase in fatigue stress (the influence of fractured fibers on total energy dissipation during fatigue was not included in the analysis used to determine τ_d).

Influence of long-duration cyclic loading on interfacial shear stress. The change in interfacial shear stress was determined for the long-duration fatigue experiment which was conducted for 3.21×10^6 cycles between stress limits of 180 MPa and 10 MPa. For comparison, the interfacial shear stress was calculated using both temperature rise data (Figs. 15a and b) and the stress-strain hysteresis curves (Fig. 16). When using temperature rise data, the energy balance given by Eq. 1 is valid only after the mean crack spacing and gage-

temperature gradient across the end of the specimen gage-section, and A_{surf} and A_{cond} are the surface area of the gage-section and the cross section of the gage-section, respectively.

section temperature have stabilized. However, using hysteresis data, Eq. 1 can be used so long as the mean crack spacing corresponding to a particular hysteresis curve is known. From Fig. 15b, the temperature rise stabilized within approximately 20,000 to 30,000 cycles.[f22] The change in matrix crack spacing was not monitored during the long-duration fatigue experiment. However, for the particular loading history used, it was previously determined that the mean crack spacing in a virgin specimen reaches a plateau within approximately 20,000 cycles (see Fig. 8). With this knowledge, the matrix crack spacing present during the long-duration fatigue experiment was estimated from surface replicas taken after specimen failure, which occurred at approximately 3.21×10^6 cycles (the presence of debris along the crack faces, which prevented complete crack closure after failure, allowed the matrix cracks to be clearly identified in the surface replicas). The replicas were obtained from regions of the gage-section which were remote to the final fracture location; the mean crack spacing was 209 μm. This crack spacing is 11 μm larger than that measured for the specimen used in the constant stress-range experiments (this specimen was prefatigued at 180 MPa - see Fig. 8), and 19 μm larger than that measured after the specimen used in the variable-frequency experiments was prefatigued at 180 MPa (see Fig. 12). These differences in crack spacing are attributed to inhomogeneities in the fiber distribution present in the billet from which the test specimens were obtained.

As shown in Figs. 19a and b, the interfacial shear stress undergoes an initially rapid decrease, from over 20 MPa to approximately 5 MPa at 25,000 cycles, after which a gradual recovery to approximately 7 MPa occurs prior to specimen failure at 3.21×10^6 cycles (note

[f22]For a given composite system the rate at which the temperature rise stabilizes depends upon the applied stress range and prior loading history of the specimen. For pre-fatigued specimens, the temperature rise can stabilize in as few as 5,000 cycles - see Fig. 13.

that these these interfacial shear stress values are based upon calculations made using the hysteresis data). The *initial* decrease in interfacial shear stress is attributed to a rapid wear process that occurs along interfacial slip-zones through the repeated frictional sliding of fibers. Jero and Kerans[21] and Mackin et al[22] have proposed that interfacial wear is a likely mechanism of fatigue damage in fiber-reinforced composites. It has been suggested that surface roughness along the fiber-matrix interface controls the rate of interfacial wear during the cyclic loading of ceramic matrix composites.[21] The decrease in interfacial shear stress which was found in the present investigation provides clear experimental evidence for a wear mechanism during the initial stages of fatigue loading.

As mentioned earlier, both the interfacial shear stress and cyclic stress-strain modulus showed a partial recovery during long duration fatigue. The calculated increase in interfacial shear stress from 5 MPa to 7 MPa would increase the average modulus by approximately 8 GPa, in good agreement with the 6.5 GPa recovery in modulus which was experimentally observed. Although speculative at this time, the partial recovery in interfacial shear stress which occurs during long-duration fatigue may be the result of time-dependent interaction with humidity in the test environment. This speculation is based upon results from fiber-pushout experiments conducted by Strevell and Jero[23], which indicate that after initial fiber debonding the frictional shear stress in SCS-6/borosilicate glass composites increased upon subsequent exposure of the composite to humid environments.

Implications of frictional heating for the use and microstructural design of ceramic matrix composites. Certain results obtained from this study have important implications regarding the use and microstructural design of ceramic matrix composites:

1. The microstructures that impart high toughness to ceramic matrix composites (relatively weak interfacial bond strength and generous fiber pullout lengths) will be the most susceptible to frictional heating. Frictional heating will also be influenced by such microstructural parameters as the type of fiber coating and the temperature dependence of mismatch in thermal expansion coefficients between the fiber and matrix.

2. Fatigue loading can cause a rapid decrease in interfacial shear stress during the initial stages of fatigue. It is expected that the rate of decrease of interfacial shear stress will be influenced by such parameters as ambient temperature and loading frequency. both of which will influence the rate of interfacial wear. The decrease in interfacial shear stress found during the initial stages of fatigue loading will result in a cycle dependence of such properties as toughness and strength. Although the interfacial shear stress was found to be approximately constant over the range of 5 Hz to 25 Hz, additional work is required to determine if this trend will persist at higher loading frequencies where the change differential thermal expansion would be expected to influence the frictional shear stress.

3. As a consequence of differential thermal expansion between the fiber and matrix, it is expected that the mechanical behavior and thermophysical properties of fiber-reinforced ceramics will be influenced by loading frequency. This frequency dependence of properties will need to be accounted for in the design of structures and components. Since the extent of frictional heating will be influenced by many variables, including fiber volume fraction and lay up, interfacial coatings, loading history and operating temperature, extensive experimental testing will be required to quantify the changes in properties which occur during fatigue.

4. The correlation of frictional heating with matrix cracking and fiber debonding raises the interesting possibility that temperature rise information can be used to assess the initial damage state of ceramic composite panels or components. Monitoring temperature rise may also be a feasible method for determining the integrity and evolving damage state of structural components.

Finally, it should be mentioned that not all ceramic composites undergo internal heating of the magnitude observed in Nicalon™/CAS-II and C_f/SiC[10] composites. For example, unpublished work by the authors has shown that cross-ply Nicalon™/SiC composites processed by chemical vapor infiltration exhibit only minimal frictional heating during tension-tension fatigue loading (at a peak stress of 160 MPa the temperature rise was typically less than 5 K at loading frequencies up to 75 Hz).

V.4 Conclusions

Based upon the results obtained from tension-tension fatigue experiments performed in air at ambient temperature, the following conclusions can be made regarding frictional heating and dynamic interfacial shear stress in 16-ply unidirectional Nicalon/CAS-II composites with 35 vol. % fibers:

1. The onset of frictional heating during cyclic loading coincides with the initiation of matrix cracking. Frictional heating and matrix cracking began at a peak stress of 120 MPa, which is approximately 50% *below* the initial monotonic proportional limit strength of the composite, indicates that fatigue damage in fiber-reinforced ceramics can occur at stress levels well below the monotonic proportional limit. This early fatigue damage has important implications

regarding the use of these composites in high-temperature oxidizing environments.

2. For a constant loading frequency and matrix crack spacing, the maximum temperature rise exhibits an approximately linear dependence on stress range or strain range. Increasing the stress range by 20 MPa resulted in an average temperature increase of approximately 3.2 K. For a fixed stress range, the temperature rise showed only a weak dependence on maximum fatigue stress. For example, at a stress range of 90 MPa, a change in peak stress from 100 MPa to 180 MPa resulted in less than a 1 K change in specimen temperature. These results suggest that the extent of internal heating is controlled primarily by the relative sliding distance of fibers within the matrix.

3. For a given peak fatigue stress and stress range, the extent of frictional heating increases as the average matrix crack spacing decreases. At a loading frequency of 75 Hz and peak stress of 160 MPa ($\Delta\sigma$ = 150 MPa), the temperature rise ranged from 28 K at a crack spacing of 228 μm, to approximately 50 K at a crack spacing of 181 μm. At a crack spacing of 181 μm, the temperature rise exceeded 100 K at a peak stress of 220 MPa ($\Delta\sigma$ = 210 MPa) and loading frequency of 75 Hz.

4. The frictional shear stress along the fiber/matrix interface undergoes a significant reduction during the initial stages of fatigue. During long duration fatigue at a loading frequency of 25 Hz and peak stress of 180 MPa, the dynamic interfacial shear stress showed an initially rapid decrease in the first 20,000 cycles (from approximately 20 MPa to 5 MPa), followed, after several million cycles, by a partial recovery to about 7 MPa. In parallel with the increase in interfacial shear stress, a partial recovery in the cyclic stress-strain modulus was observed.

The magnitude of the modulus increase was consistent with analytical predictions which were based upon the observed increase in interfacial shear stress.

5. A gradual decay in temperature rise was observed during long-duration fatigue loading. The temperature rise ($T - T_{ambient}$) decreased from a maximum of approximately 18 K at 30,000 cycles to 15 K after 3.16×10^6 cycles. This decrease in temperature is attributed in part to the modulus recovery which occurs during cyclic loading; under load-controlled fatigue, a modulus increase causes a proportional reduction in strain range ($\Delta\varepsilon = \Delta\sigma/E_C$) and, hence, a reduction in the frictional sliding distance of fibers. The interfacial shear stress was not significantly influenced by loading frequency; for a given crack spacing, there was less than a 1 MPa change in shear stress for loading frequencies between 5 and 25 Hz.

6. The occurrence of frictional heating and the cycle dependent change in frictional shear stress have important implications regarding the role of the fiber/matrix interface in fatigue and the use of ceramic composites in applications involving fatigue loading. In particular, differential thermal expansion between the fiber and matrix during cyclic loading may result in a frequency dependence of properties which are influenced by the degree of contact between the fiber and matrix; such as interfacial wear and mechanical properties such as toughness, damping and fatigue life. Thermophysical properties such as thermal conductivity are also expected to be influenced by loading frequency.

V.5 References

1. D. B. Marshall and A. G. Evans, "Failure Mechanisms in Ceramic-Fiber/Ceramic-Matrix Composites," *J. Am. Ceram. Soc.*, **68** [5] 225-31 (1985).

2. E. Minford and K. M. Prewo, "Fatigue of Silicon Carbide Reinforced Lithiumalumino-Silicate Glass-Ceramics," in Tailoring Multiphase and Composite Ceramics, C. G. Patano and R. E. Messing, Eds., Plenum Publishing Corporation, New York, 1986, pp. 561-70.

3. K. M. Prewo, "Fatigue and Stress Rupture of Silicon Carbide Fibre-Reinforced Glass-Ceramics," *J. Mater. Sci.*, **22** 2695-2701 (1987).

4. J. W. Holmes, "Influence of Stress-Ratio on the Elevated Temperature Fatigue Life of a SiC Fiber-Reinforced Si_3N_4 Composite," *J. Am. Ceram. Soc.*, **74** [7] 1639-45 (1991).

5. S. Shuler and J. W. Holmes, "Influence of Frequency on the Fatigue Life of a C-Fiber SiC-Matrix Composite," *J. Am. Ceram. Soc.*, submitted for publication.

6. D. B. Marshall and W. C. Oliver, "Measurement of Interfacial Mechanical Properties in Fiber-Reinforced Ceramic Composites," *J. Am. Ceram. Soc.*, **70** [8] 542-48 (1987).

7. B. N. Cox, "Interfacial Sliding near a Fibrous or Layered Composite During Thermal Cycling", *Acta. Metall. Mater.*, **38** [12] 2411 - 24 (1990).

8. R. M. McMeeking and A. G. Evans, "Matrix Fatigue Cracking in Fiber Composites," *Mechanics of Materials*, **9** 217-27 (1990).

9. T. Kotil, J. W. Holmes and M. Comninou, "Origin of Hysteresis Observed During Fatigue of Ceramic Matrix Composites," *J. Am. Ceram. Soc.*, **73** [7] 1879-83 (1990).

10. J. W. Holmes and S. F. Shuler, "Temperature Rise During Fatigue of Fibre-Reinforced Ceramics," *J. Mater. Sci. Lett.*, **9** [11] 1290-91 (1990).

11. J. W. Holmes and C. Cho, "Frictional Heating in a Fiber-Reinforced Ceramic Composite," *J. Mater. Sci. Lett.*, in press.

12. J. W. Holmes, "A Technique for Tensile Fatigue and Creep Testing of Fiber-Reinforced Ceramics," *J. Comp. Mater.*, to appear in January 1992 issue.

13. L. Butkus and L. Zawada, "Room Temperature Tensile and Fatigue Properties of Silicon-

Carbide Fiber-Reinforced Ceramic Matrix Composites," presented at Aeromat '90, Long Beach, CA, May 21-24, 1990.

14. J. Aveston and A. Kelly, "Theory of Multiple Fracture of Fibrous Composites," *J. Mater. Sci.*, **8** 352-62 (1973).

15. B. Budiansky, J. W. Hutchinson, and A. G. Evans, "Matrix Fracture in Fiber-Reinforced Ceramics," *J. Mech. Phys. Solids*, **34** [2] 167-89 (1986).

16. C. Cho, J. W. Holmes, and J. R. Barber, "Distribution of Matrix Cracks in a Uniaxial Composite," *J. Am. Ceram. Soc.*, to appear in January 1992 issue.

17. P. Karandikar , R. Talreja, and T.-W. Chou, "Evolution of Damage and Mechanical Response of Ceramic Matrix Composites," submitted to *J. Mater. Sci.* (1991)

18. C. Cho and J. W. Holmes, "Influence of fatigue Loading and Test Frequency on Interfacial Shear Stress in Fiber-Reinforced Ceramics," presented at the 16th Annual Conference on Composites and Advanced Ceramics, Cocoa Beach, FL, January 7-10, 1992 Paper. No. 50-C-92F.

19. C. Cho, J. W. Holmes, and J. R. Barber, "Estimation of Interfacial Shear in Fiber-Reinforced Ceramics from Frictional Heating Measurements," *J. Am. Ceram. Soc.*, **74** [11] 2802-808 (1991).

20. V. Ramakrishnan, J. W. Holmes and M. Comninou," High-Frequency Fatigue and Internal Heating in Fiber-Reinforced Ceramics," presented at the 16th Annual Conference on Composites and Advanced Ceramics, Cocoa Beach, FL, January 7-10, 1992 Paper. No. 51-C-92F.

21. P. D. Jero and R. J. Kerans, "Effect of Interfacial Roughness on the Frictional Stress Measured Using Pushout Tests," **74** [11] 2793-801 (1991).

22. T. J. Mackin, P. D. Warren and A. G. Evans, "Fiber Pushout of a Fatigued Specimen," presented at the 93rd Annual ACS Meeting, Cincinnati, OH, April 28 - May 2, 1991, Paper No. 54-SVI-91.

23. R. J. Strevell and P. D. Jero, "Effect of Moisture on the Fiber/Matrix Bond Strength and Sliding Friction in a Glass Matrix Composite," presented at the 93rd Annual Meeting, Cincinnati, OH, April 28 - May 2, 1991, Paper No. 64-SVI-91.

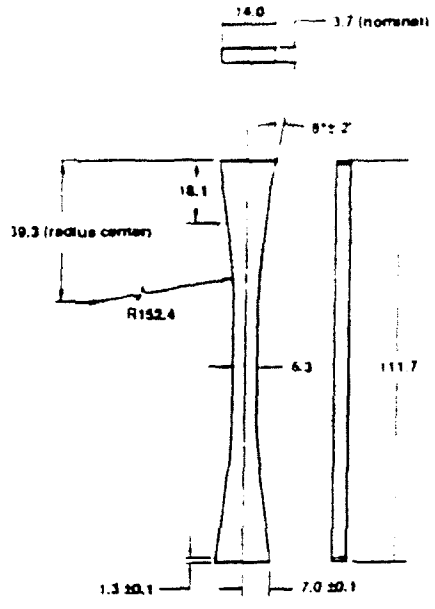

Fig. 1. Specimen geometry used to investigate frictional heating during the tensile-fatigue of ceramic matrix composites. All dimensions are given in millimeters.

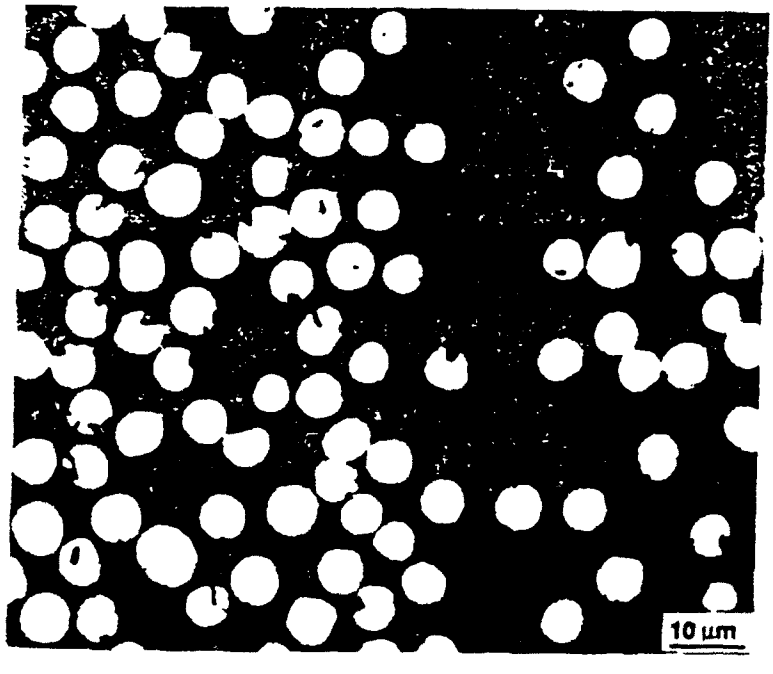

Fig. 2. Optical micrograph showing typical fiber-distribution in the $[0]_{16}$-Nicalon™/CAS-II specimens. The composite had a nominal fiber fraction of 35 vol. %.

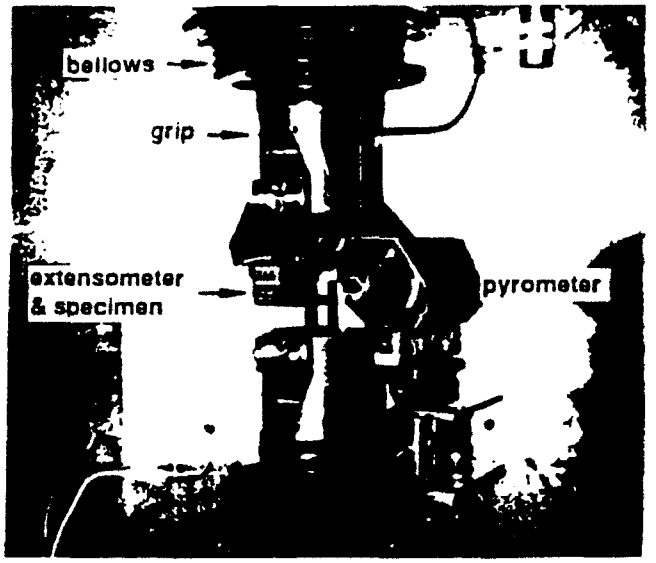

Fig. 3. Experimental arrangement used to investigate frictional heating in fiber-reinforced ceramics. The isothermal test chamber, which completely surrounded the specimen and grips, had a volume of 0.025 m^3. The temperature within the chamber was controlled to 293 ±0.1K by circulating water through the chamber walls.

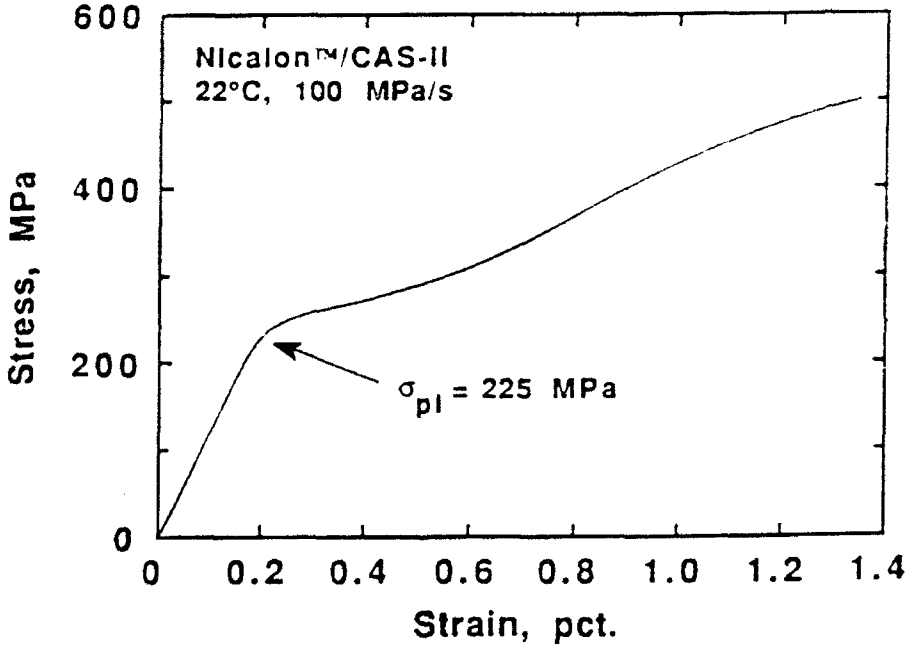

Fig. 4. Monotonic tensile behavior of $[0]_{16}$-Nicalon™/CAS-II at 293 K.

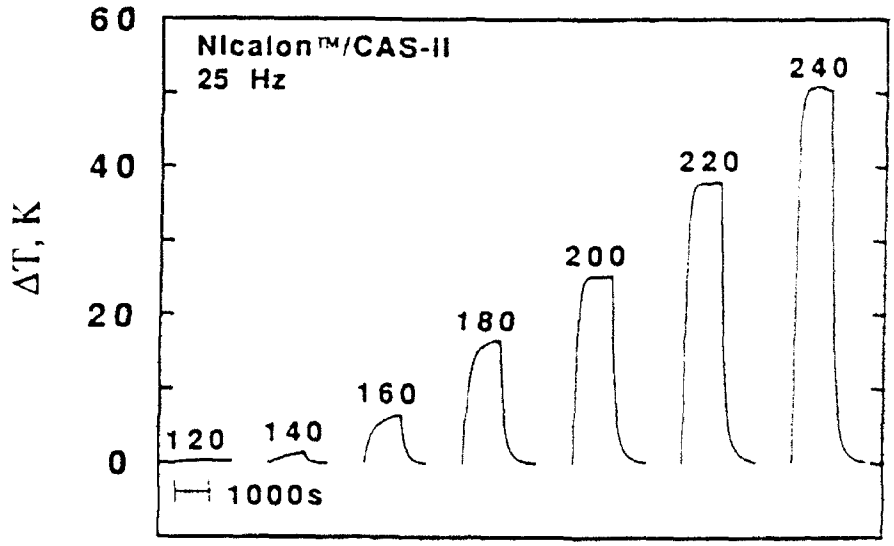

Fig. 5. Influence of stress range on temperature rise. Fixing the minimum fatigue stress at 10 MPa, the maximum fatigue stress was increased in 20 MPa increments from 100 MPa to 240 MPa. The specimen was fatigued for 1000 s at each stress level. Coinciding with the initiation of matrix cracking, a temperature rise of 0.3 K was first detected at a stress of 120 MPa. The initial temperature of the composite was 293 K. From Holmes and Cho [8].

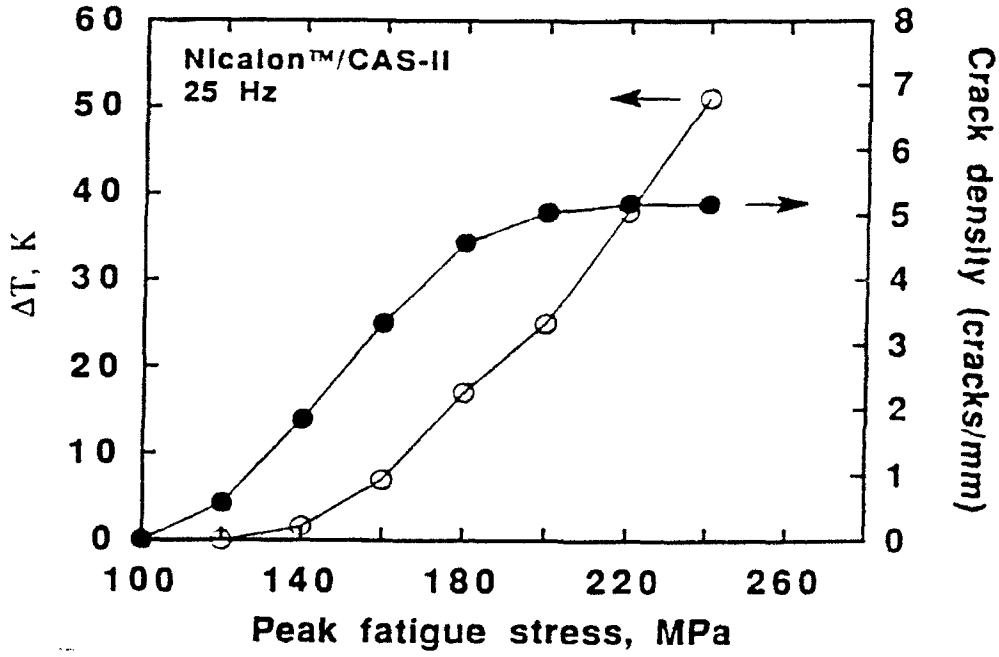

Fig. 6. Temperature rise and matrix crack density (reciprocal of mean crack spacing) versus maximum fatigue stress. The crack density reached an approximate plateau above 200 MPa. For all loading histories, the loading frequency was 25 HZ and the minimum fatigue stress was 10 MPa. The initial temperature of the composite was 293 K. After Holmes and Cho [8].

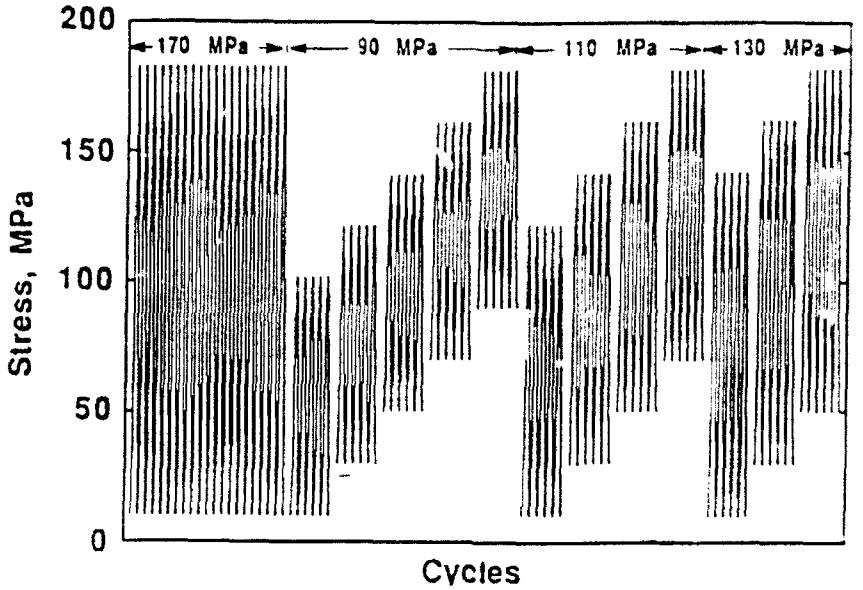

Fig. 7. Loading history used to investigate the influence of stress range ($\Delta\sigma$) and maximum fatigue stress on temperature rise. To achieve a constant crack density, the specimen was first prefatigued for 100,000 cycles at 25 Hz between fixed stress limits of 180 MPa and 10 MPa. Each constant stress-range experiment was conducted for 25,000 cycles at a loading frequency of 25 Hz. The stress range is given above each group of fatigue loading blocks.

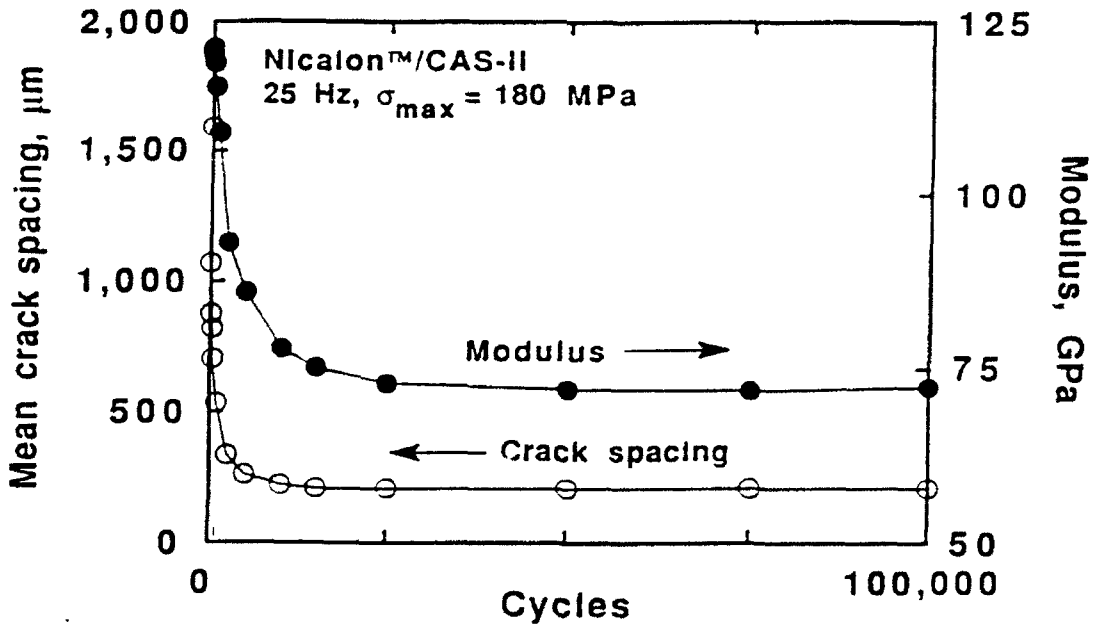

Fig. 8. Change in matrix crack spacing and cyclic stress-strain modulus during fatigue at 25 Hz between fixed stress limits of 180 MPa and 10 MPa. Note that a stable crack density was achieved within approximately 20,000 cycles. For this loading history, the modulus reached an approximate plateau between approximately 25,000 and 30,000 cycles.

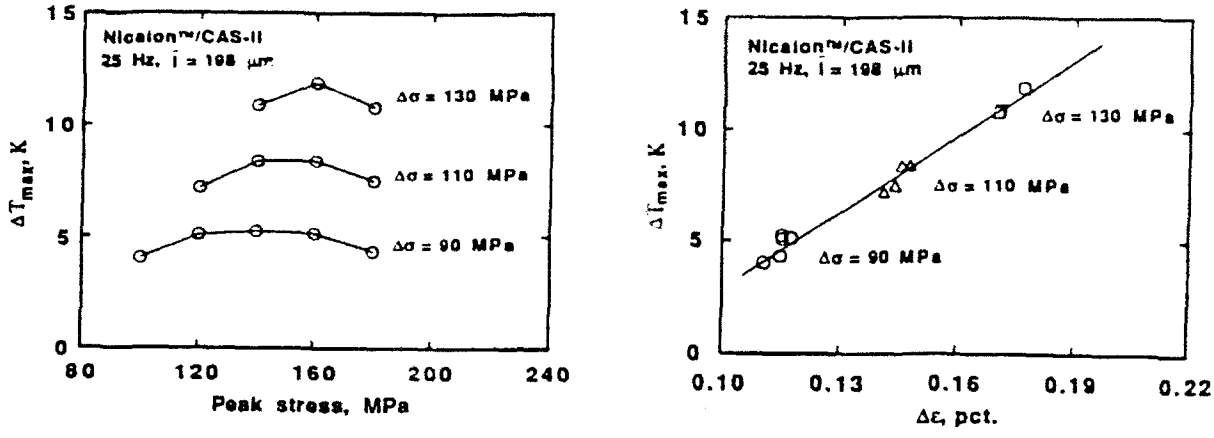

(a) ΔT_{max} versus $\Delta\sigma$. (b) ΔT_{max} versus $\Delta\varepsilon$.

Figs. 9a and b. (a) Influence of stress range ($\Delta\sigma$) and maximum fatigue stress on temperature rise. For a given stress range, the temperature rise exhibits a weak dependence on peak fatigue stress. (b) Relationship between maximum temperature rise and strain range. The approximately linear relationship between temperature rise and strain range suggests a mechanism of internal heating involving the frictional slip of fibers. The loading history is shown in Fig. 7.

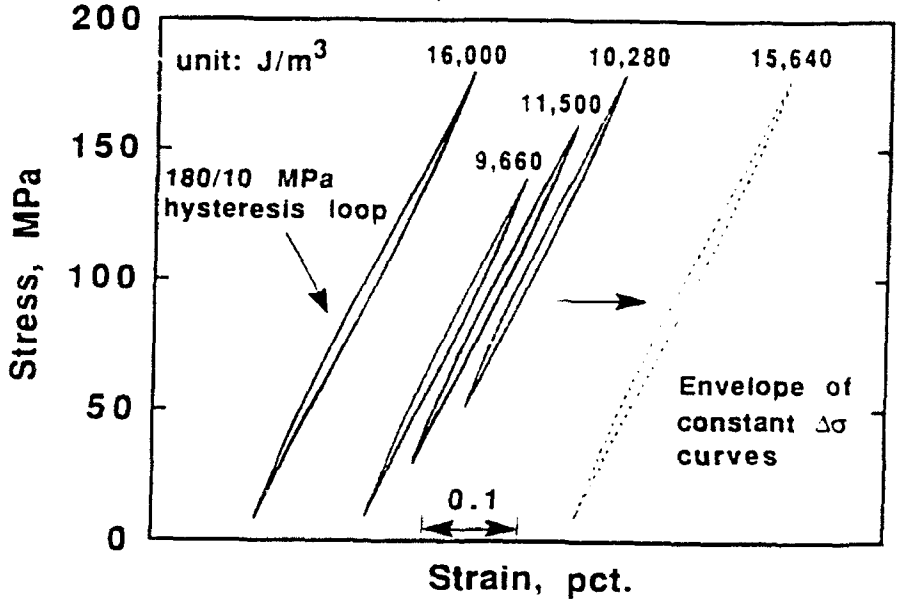

Fig. 10. Stress-strain hysteresis curves obtained after 100,000 cycles of "pre-fatigue" between stress limits of 180 MPa and 10 MPa and during subsequent fatigue experiments conducted at a stress-range of 130 MPa (the peak stresses were 140, 160 and 180 MPa - see Fig. 7). The constant stress range curves have been separated for clarity. Corresponding to the peak in temperature rise (Fig. 9a), the energy dissipation was a maximum at an intermediate level of peak fatigue stress. To the right is the hysteresis envelope formed by overlaying the three constant stress range curves.

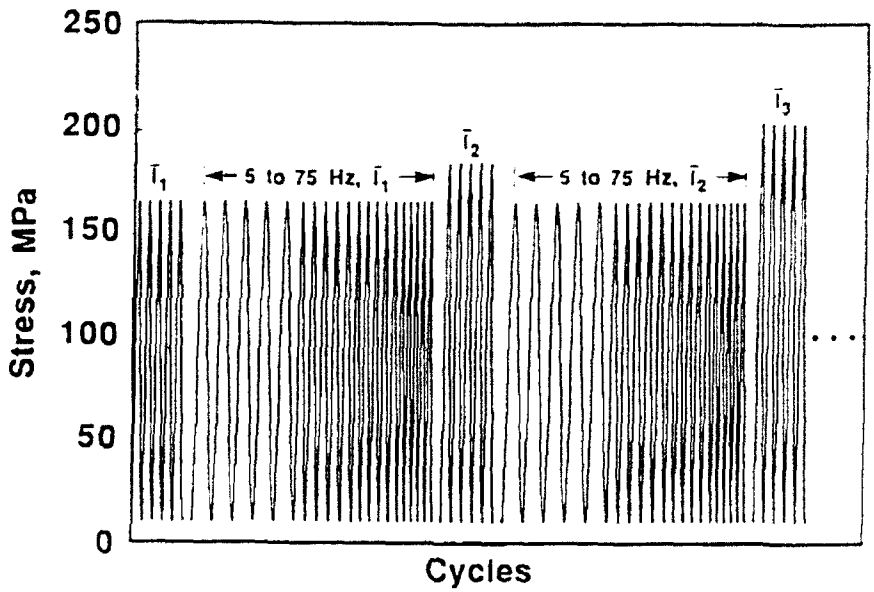

Fig. 11. Loading sequence used to investigate the influence of test frequency and matrix crack spacing on temperature rise. To change the crack spacing, the maximum fatigue stress was sequentially increased; maximum stresses of 160, 180, 200 and 220 MPa were employed (in all instances, the specimen was fatigued for 50,000 cycles at 25 Hz - the minimum cycle stress was 10 MPa). For each crack spacing, the specimen was sequentially subjected to fatigue at loading frequencies of 5, 10, 25, 50 and 75 Hz; the specimen was fatigued for 1000 s at each frequency.

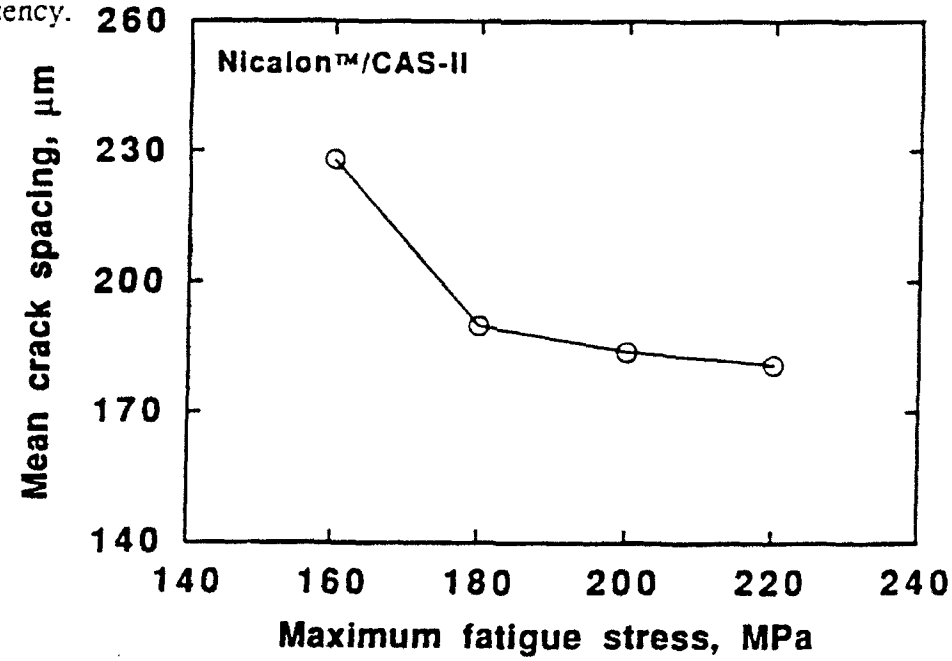

Fig. 12. Matrix crack spacing versus maximum fatigue stress. At each stress, fatigue was conducted for 50,000 cycles at a frequency of 25 Hz and a minimum stress of 10 MPa (see Fig. 11).

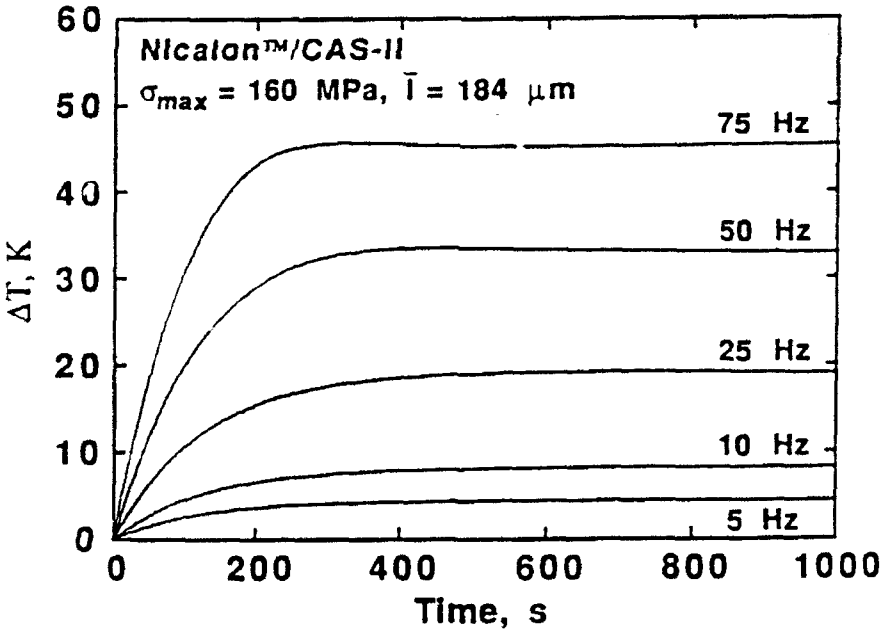

Fig. 13. Typical temperature rise curves obtained from fatigue experiments conducted at loading frequencies of 5 to 75 Hz between fixed stress limits of 160 MPa and 10 MPa. The specimen was previously fatigued at 25 Hz for 50,000 cycles between stress limits of 200 MPa and 10 MPa; this provide an average matrix crack spacing of 184 μm.

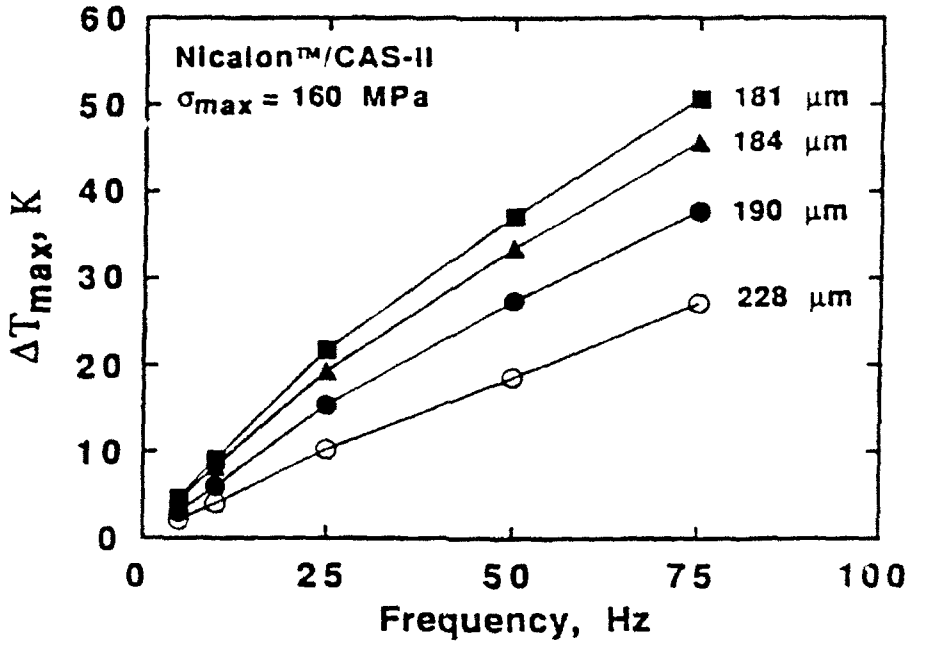

(a) Temperature rise versus frequency and crack spacing.

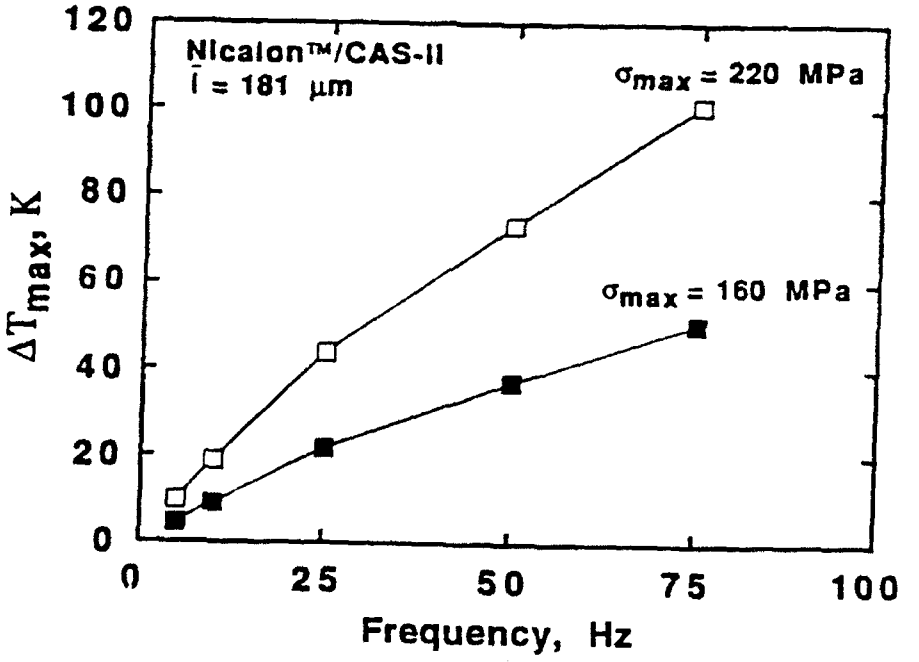

(b) Temperature rise versus frequency and fatigue stress.

Figs. 14a and b. (a) Influence of average matrix crack spacing and loading frequency on maximum temperature rise at a fixed stress range (the experiments were conducted between fixed stress limits of 160 MPa and 10 MPa - see Fig. 11). (b) Influence of stress range and loading frequency on temperature rise at a constant crack spacing (for both fatigue stresses the minimum cycle stress was 10 MPa).

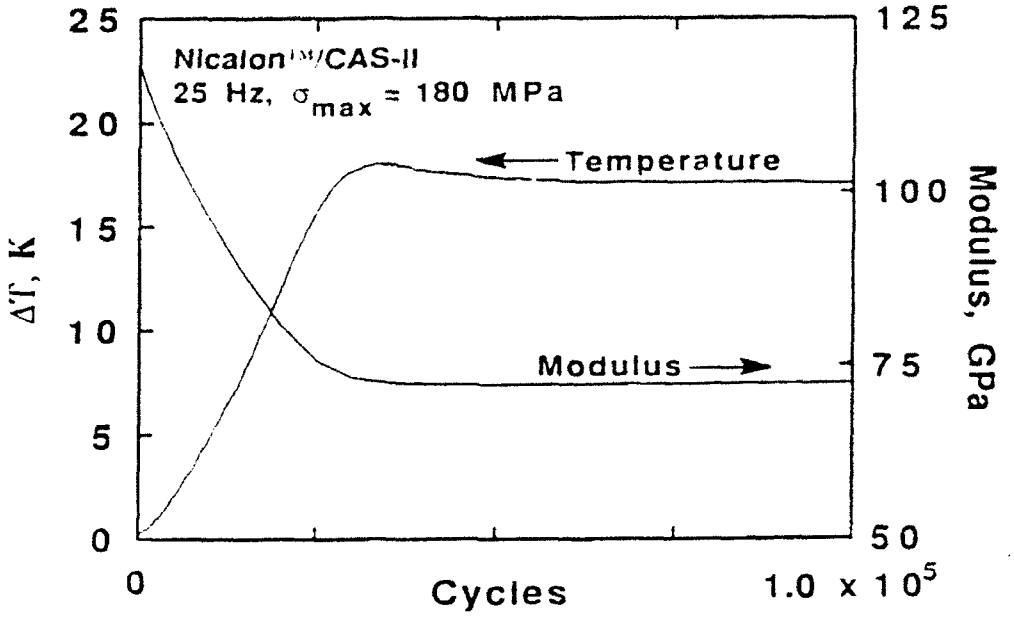

(a) Initial portion of curves.

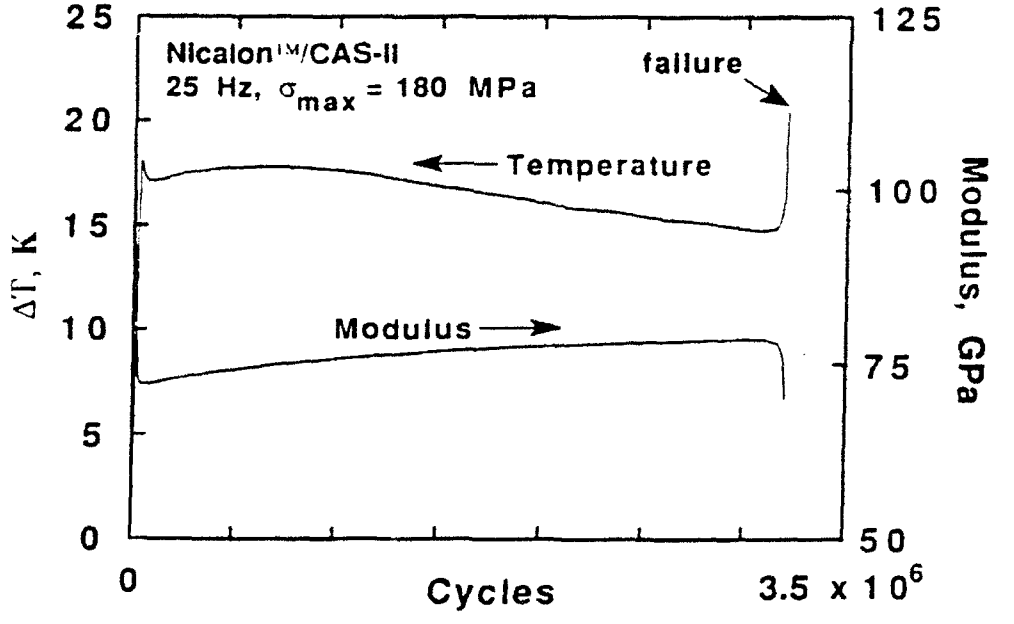

(b) Temperature rise and modulus curves up to failure.

Figs. 15a and b. Influence of long-duration cyclic loading on temperature rise and cyclic stress-strain modulus. The experiment was conducted at a loading frequency of 25 Hz between fixed stress limits of 180 MPa and 10 MPa. (a) The modulus rapidly decreased within the first 30,000 cycles of fatigue. (b) With further fatigue, a partial recovery in modulus and gradual decay in temperature occurred. Failure occurred at approximately 3.21 x 10^6 cycles.

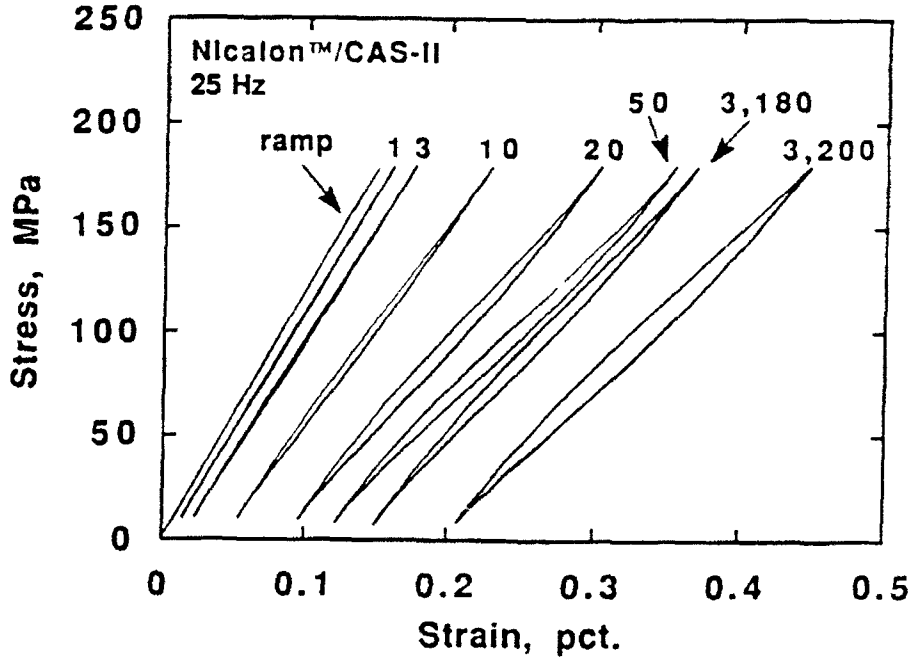

Fig. 16. Change in hysteresis behavior during the long duration fatigue of unidirectional Nicalon/CAS-II. The experiment was conducted at 25 Hz between fixed stress limits of 180 MPa and 10 MPa. The numbers above each curve give the fatigue cycles in thousands. Specimen failure occurred at approximately 3.21 x 10^6 cycles.

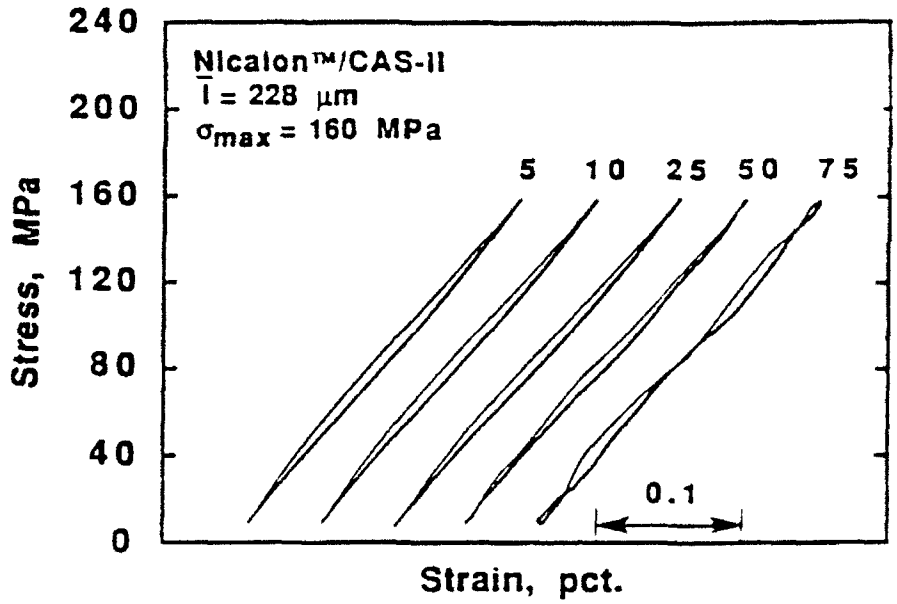

(a) $\bar{l}$ = 228 μm

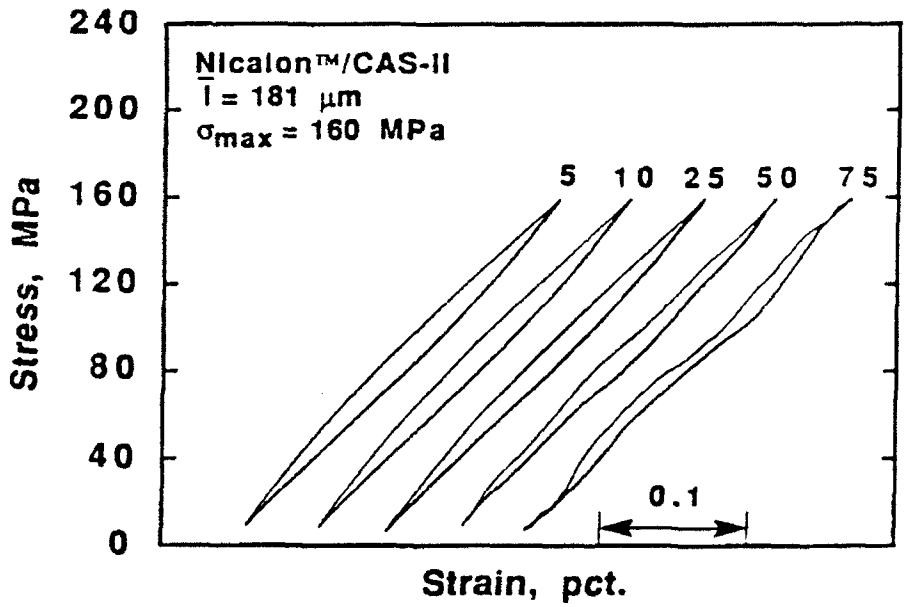

(b) $\bar{l}$ = 181 μm

Figs. 17a and b. Influence of loading frequency on the cyclic stress-strain response of $[0]_{16}$-Nicalon/CAS-II. The hysteresis loops were obtained at the end of each 1000 s test. The numbers above each curve correspond to the sinusoidal loading frequency in Hz. The distortion of the hysteresis curves at 50 and 75 Hz is attributed to compliance of the load-frame.

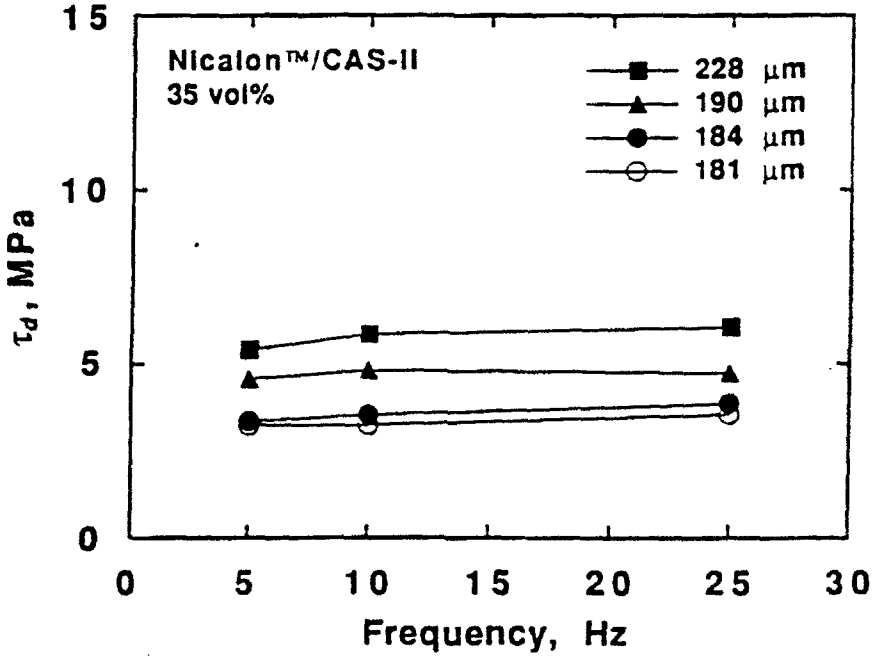

Fig. 18. Influence of loading frequency and mean crack spacing on dynamic interfacial shear stress, τ_d. The temperature rise data shown in given in Fig. 14a were used in the analysis.

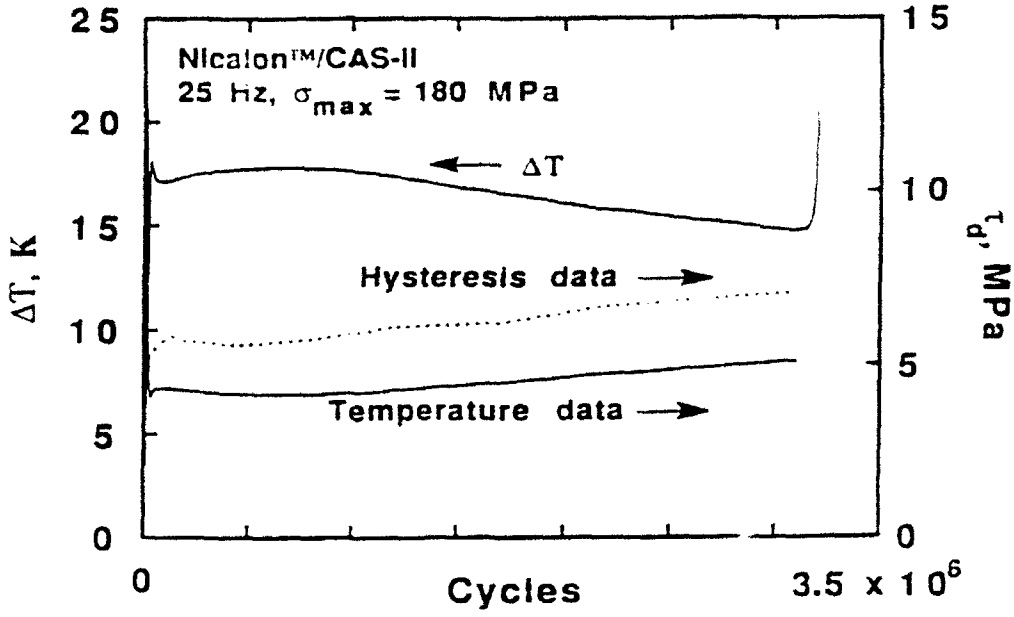

(a) Interfacial shear up to 3.18 x 10^6 cycles.

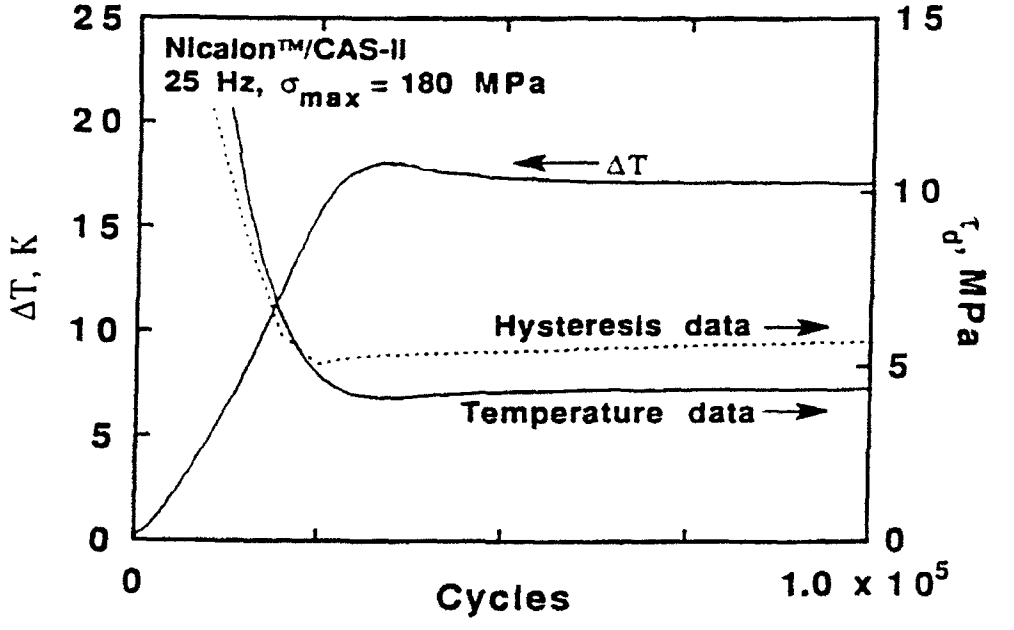

(b) Initial portion of curves.

Figs. 19a and b. Change in interfacial shear during long duration cyclic loading between fixed stress limits of 180 MPa and 10 MPa. For comparison, the interfacial shear was calculated using the temperature rise data given in Fig. 15 and stress-strain hysteresis data (several of the hysteresis curves are shown in Fig. 16). Specimen failure occurred at 3.21 x 10^6 cycles.